Continuous Electropermutation using Ion-Exchange Textile

by

Carl-Ola Danielsson
Department of Mechanics

November 2004
Technical Reports from
Royal Institute of Technology
Department of Mechanics
S-100 44 Stockholm, Sweden

Typsatt i $\mathcal{AMS}$-LaTeX.

Akademisk avhandling som med tillstånd av Kungliga Tekniska Högskolan i Stockholm framlägges till offentlig granskning för avläggande av teknologie licentiatexamen fredagen den 19:de november 2004 kl 10.15 i seminarierum S40, Kungliga Tekniska Högskolan, Teknikringen 8, Stockholm.

Universitetsservice US AB, Stockholm 2004

Continuous Electropermutation Using Ion-Exchange Textile

Carl-Ola Danielsson
Department of Mechanics, Royal Institute of Technology
SE-100 44 Stockholm, Sweden.

Abstract

Increased levels of nitrate in ground water has made many wells unsuitable as sources for drinking water. In this thesis an ion-exchange assisted electro-membrane process, suitable for nitrate removal, is investigated both theoretically and experimentally. A new ion-exchange textile material is introduced as a conducting spacer in the feed compartment of an continuous electropermutation cell. The ion-exchange textile have a high permeability and provides faster ion-exchange kinetics compared to ion-exchange resins. The sheet shaped structure of the textile makes it easy to incorporate into the cell.

A report on the development of a new electro-membrane module, capable of incorporating an ion-exchange textile spacer, is presented. A theoretical study of the flow field through the electro-membrane module was performed using two different 2-D models. The calculated flow distributions provided by different proposed module designs were compared and a prototype module was produced. The flow field obtained with the prototype cell was visualised in a experimental cell with a transparent plexiglass cover.

A steady-state model based on the conservation of the ionic species is developed. The governing equations on the microscopic level are presented and volume averaged to give macro-homogeneous equations. The model equations are analysed and relevant simplifications are motivated and introduced. The dimensionless parameters governing the continuous electropermutation process are identified and their influence on the process are discussed. The mathematical model can be used as a tool when optimising the process parameters and designing equipment.

An experimental study that aimed to show the positive influence of using the ion-exchange textile in the feed compartment of an continuous electropermutation process is presented. The incorporation of the ion-exchange textile significantly improves the nitrate removal rate at the same time as the power consumption is decreased. A superficial solution of sodium nitrate with a initial nitrate concentration of 105 ppm was treated. A product stream with less than 20 ppm nitrate could be obtained, in a single pass mode of operation. Its concluded from these experiments that continuous electropermutation using ion-exchange textile provides an interesting alternative for nitrate removal, in drinking water production. The predictions of the mathematical model are compared with experimental results and a good agreement is obtained.

Descriptors: Ion-exchange textile, Ion-exchange membrane, Electropermutation, Electroextraction, Electrodialysis, Electrodeionisation, Modeling, Conducting spacer, Nitrate removal, Water treatment.

Preface

This thesis treats continuous electropermutation both theoretically and experimentally. The thesis is based on the following pappers:

Paper 1. Carl-Ola Danielsson, Anna Velin, Anders Dahlkild & Mårten Behm 2004 Design of Electrodialysis module. *Technical report*

Paper 2. Carl-Ola Danielsson, Anders Dahlkild, Anna Velin & Mårten Behm 2004 Modelling Nitrate Removal by Electropermutation Using Non-selective Ion-Exchange Textile as Conducting Spacer. *To be submitted*

Paper 3. Carl-Ola Danielsson, Anna Velin, Mårten Behm & Anders Dahlkild 2004 Experimental work on Nitrate Removal by Electropermutation using Ion-Exchange Textile as Conducting Spacer. *To be submitted*

Division of work between authors

The work presented in this thesis has been done in collaboration with other researchers. The respondent has performed the major part of the work. Docent Anders Dahlkild, Department of Mechanics KTH, Dr. Anna Velin, Vattenfall Utveckling AB and Dr. Mårten Behm, Division of Applied Electrochemistry KTH, have acted as supervisors. They have all contributed with comments and discussion of the the work and the manuscripts.

Parts of the modeling activities have been presented in a poster at,
The 53rd Annual Meeting of the International Society of Electrochemistry, Düsseldorf, Germany, in September 2002,
and in a talk given at,
The 205th meeting of the electrochemical society in San Antonio, Texas, U.S., in May 2004.

Contents

CHAPTER 1

Introduction

Obtaining clean freshwater from the tap is something that many of us take for granted. We use it every day to prepare our food, to wash our clothes and for many other applications. In Sweden the consumption of water is about 200 l of water per person per day (Hult 1998). Increasing environmental pollution has made many wells unsuitable as freshwater sources. Use of water treatment techniques is needed in order to meet society's need of high quality water.

What is regarded as good water quality depends on the application. Potable water should be free from toxic and harmful substances. Ultrapure water on the other hand, is not considered as high quality drinking water, where some minerals are desirable. The taste, smell and visual appearance of the water are other important aspects of drinking water quality. Furthermore there are some technical aspects that are considered in drinking water production. The pH of the water is often increased in order to reduce corrosion problems in the pipes.

The definition of clean water in many industrial applications is something completely different compared to the potable water. The electronic and pharmaceutical industries require extremely pure water in their processes. In powerplants high-purity water is used to reduce problems with corrosion that could be a serious problem at the temperatures and pressures present in the boilers. The production of this ultrapure water requires sophisticated water treatment systems.

Water treatment systems are also used in the industry to reduce discharge of e.g. heavy metals for environmental reasons. There might also be an economical advantage to recycle chemicals used in the process. In many industrial areas a zero waste target is on the agenda.

In this thesis a special electro-membrane technique, combined with a new textile ion-exchange material, is investigated. This technique is capable of removing ionic compounds from water with low conductivity. A product stream free from the removed ions and a concentrated waste stream are generated. The concentrated waste stream can be treated with other techniques or, depending on the application, the concentrate might be recycled. The specific application studied in this thesis is nitrate removal from ground water to produce drinking water.

1.1. Background

The research presented has been conducted in close collaboration with Vattenfall Utveckling AB(VUAB) one of the industrial partners involved within FaxénLaboratoriet. The electrochemistry group of Vattenfall had been engaged to develop an efficient system for nitrate elimination/reduction to purify ground and industrial waters. The system was based on the integration of conventional ion exchange technique for nitrate removal with selective electrochemical nitrate reduction. Part of this nitrate program was the participation in the EU funded research project Iontex (Schoebesberger *et al.* 2004).

The purpose of Iontex was to develop new functionalised textile materials made from cellulosic fibers. VUAB's task was to develop an electrodialysis module which could incorporate a textile with ion-exchange properties. To achieve this theoretical and experimental studies were conducted and the results form these are presented in this thesis.

1.2. Outline of thesis

This thesis consists of two parts. The first part is to give a background and overview of the work presented in the second part.

The problem with nitrate in ground water and different alternatives for nitrate removal is discussed in the second chapter. In the third chapter the Iontex project and in particular VUAB's activities are presented. In chapter four a short introduction to the modeling is given. The basic idea behind volume-averaging to obtaining macro-homogeneous transport equations in a porous media is described. Chapter five gives an overview of the main results presented in the second part of this thesis.

CHAPTER 2

Nitrate Removal

The primary health concern regarding nitrate, NO_3^-, is that it is reduced to nitrite, NO_2^-, in the body. Nitrite in turn reacts with the red blood cells to form methemoglobin which affects the blood's capability to transport oxygen. Infants are especially sensitive due to their low gastric acidity which is favorable for the reduction of nitrate. High intake of nitrate by infants e.g. when bottle-fed, can cause a condition known as "blue-baby" syndrome which can be fatal. It is also claimed by some researchers that there exist a correlation between exposure to nitrate and the risk of developing cancer. This is however still not established.

According to European Union regulations, drinking water must not contain more than 50 ppm of nitrate, although the recommended value is a concentration of less than 25 ppm (European Community 1998). German health authorities demands that the nitrate level in water used in the preparation of baby food should be less than 10 ppm Kesore *et al.* (1997). In the guidelines for drinking water quality published by WHO (2004) in 2004 the maximum level of nitrate is given as 50 mg/litre. In drinking water derived from surface water the nitrate level rarely exceeds 10 ppm; however increased nitrate concentrations in ground water have made many wells unsuitable as drinking water sources.

The accumulation of nitrate in the environment results mainly from the use of nitrogenous fertilisers and from poorly or untreated sewage. In addition, nitrate-containing wastes are produced by many industrial processes. Because agricultural activities are involved in the nitrate pollution problem, farmers and rural communities are the most threatened populations.

2.1. Nitrate removal

The removal of nitrates from water can be accomplished in a number of different ways e.g. ion exchange, biological processes or with membrane techniques. The ideal process for nitrate removal would be able to treat large volumes of water at a low cost. Furthermore it is desirable that the process adapts well to different feed loads and works without the addition of any chemicals. A review of different alternatives for nitrate removal is presented by Kapoor & Viraraghavan (1997).

2.1.1. *Biological Denitrification*

Biological denitrification is commonly used for treatment of municipal and industrial waste water. The concern of bacterial contamination of the treated water has made the transfer to production of drinking water slow. The main advantage of using biological nitrate reduction is that the nitrate is turned into nitrogen gas reducing problems with waste solutions. Biological denitrification is however quite slow and thus large installations are required. Furthermore the bacteria responsible for the transformation of nitrate into nitrogen are sensitive to changes in their working conditions. Temperature and pH has to be kept within a narrow range, this together with the need for relatively large installations makes the biological methods expensive.

2.1.2. *Ion-exchange (IX)*

A good introduction to ion-exchange technology in general is given by Helfferich (1995).

Ion-exchange for nitrate removal involves the passing of the water through a bed of nitrate selective anion-exchange resin beads. The nitrate ions present in the water are exchanged for chloride or bicarbonate ions until the the bed is exhausted. The exhausted resin then has to be regenerated using concentrated solutions of e.g. sodium chloride.

Problems with ion-exchange are related to the non-continuous mode of operation. This requires several IX columns to be installed in parallel in order to obtain a continuous production. The need for regeneration solution adds to the operational cost as well as leads to a problem of waste disposal. There are some installations where the spent regeneration solution is treated with biological denitrification.

The advantages with IX is that very low nitrate concentrations can be reached. The technique is very flexible and relatively insensitive to changes in temperature. The time needed for start up is very short and the capital cost is much less than for biological denitrification plants. Furthermore operating costs are slightly lower for IX compared to biological denitrification (Kapoor & Viraraghavan 1997).

2.1.3. *Reverse Osmosis (RO)*

Reverse Osmosis is a pressurised membrane technology. The pressure required is between 20-100 bar which makes the power consumption quite high. Common problems associated with RO membranes include fouling, compaction and deterioration with time (Mulder 1996). The reject stream from a RO unit represent between 20 and 50 % of the feed flow. This gives relatively large volumes of concentrated waste streams which poses a disposal problem (Schoeman & Steyn 2003).

2.1.4. *Ion-exchange membrane techniques.*

There are several different techniques for nitrate removal which makes use of ion-exchange membranes to achieve a nitrate separation. Examples of such are Donnan dialysis, electrodialysis, electrodeionisation and electropermutation. Salem *et al.* (1995) claim that these processes are the most suitable when large volumes of water are to be treated.

2.1.4.1. *Donnan dialysis (DD)*

The driving force in Donnan dialysis is a difference in chemical potential over an ion-exchange membrane. Nitrate removal with DD is quite slow compared to the other ion-exchange membrane techniques.

2.1.4.2. *Electrodialysis (ED)*

Electrodialysis is an electrochemical separation process which combines ion-exchange membranes and an electric field to separate ionic species from an aqueous solution. One important application for electrodialysis is desalination of brackish water to produce portable water. Electrodialysis is also used in order to increase the salt concentration e.g. before evaporation to produce table salt or for direct use in the chlor-alkali process.

In an electrodialysis stack cation(CEM) and anion(AEM) exchange membranes are alternated between two electrodes, as shown in figure 2.1. The ions in the water migrate over the membranes under the influence of the applied electric field. The treated water will become desalinated. One attractive feature of ED is that it does not require any addition of chemicals.

The relatively low conductivity of the of the water to be treated makes the power consumption for driving the electric current through the ED stack relatively high and concentration polarisation limits the intensity of the current density that can be applied.

2.1.4.3. *Continuous Electrodeionisation (CDI)*

The general idea behind CDI, is to incorporate an ion-exchange bed between the membranes in the dilute compartment of an ED cell. The ion-exchange media provides extra conductivity to the dilute compartment and reduces the problems associated with the limiting current. The most widespread application is the production of ultrapure water, used for example as feed water to boilers in power plants or as rinse water in the electronics industry.

Nitrate removal with CDI was investigated by Kesore *et al.* (1997). They found that the incorporation of a nitrate-selective ion-exchange spacer between the membranes in an electrodialysis stack reduced the energy consumption for nitrate removal compared to ED.

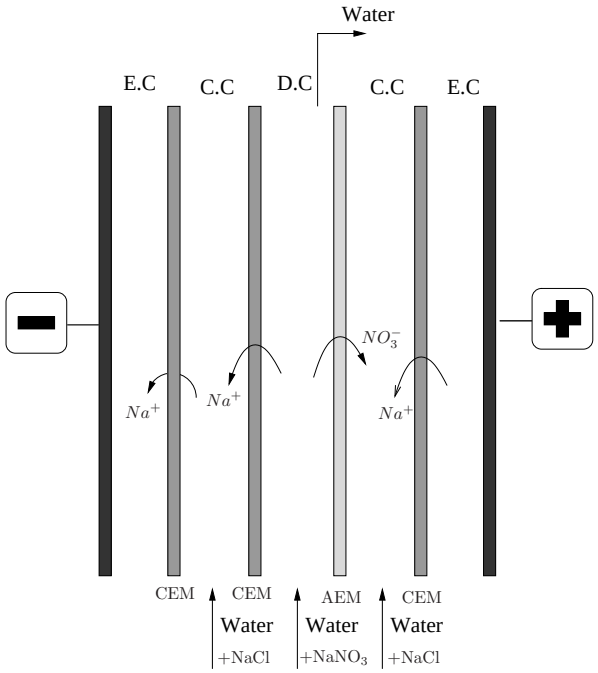

FIGURE 2.1. The principles of ED/CDI for nitrate removal. The dilute compartment of a CDI cell is filled with a bed of ion-exchange material.

2.1.4.4. *Continuous Electropermutation (CEP)*

When using ED or CDI to remove nitrate a desalinated water with very low conductivity can be obtained. This might be a unwanted feature in drinking water production, since although most of the nitrate need to be removed it is desirable to maintain the concentration of minerals. The idea with electropermutation (Ezzahar *et al.* 1996) for nitrate removal is to replace the anions in the water. This is done by replacing the cation exchange membranes in a CDI stack with anion-exchange membranes. The water to be treated is fed through the feed compartment which is filled with an anion-exchange material. On each side of the feed compartment are concentrate compartments with high concentration of e.g. chloride Cl^-. The dilute and concentrate compartments are separated by anion exchange membranes. The advantage of CEP compared to CDI and ED is that all cations are preserved. Also in CEP, the total volume of the ion-exchange bed can be used to capture and transport nitrate whereas in EDI only a fraction of the bed is designated to exchange anions and participate in the nitrate removal process. Furthermore the conductivity of the water does not change significantly. The main drawback is that salt needs to be added to compensate for the anions that are used to replace nitrate.

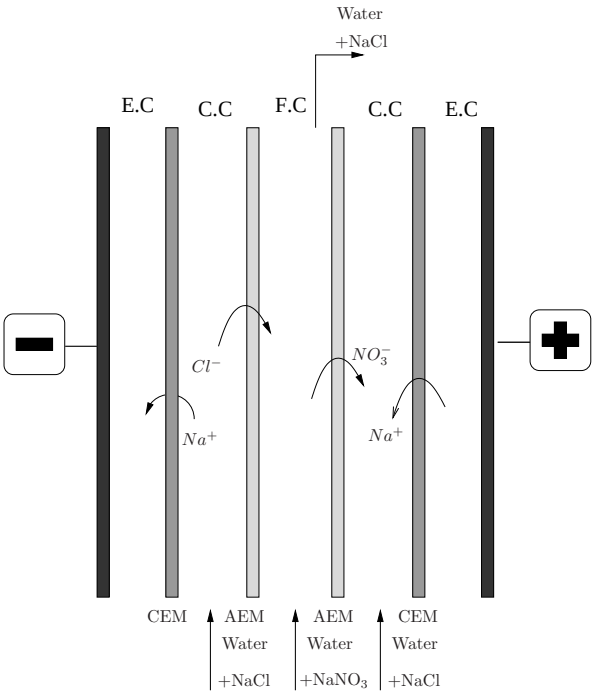

FIGURE 2.2. The principles of continuous electropermutation for nitrate removal.

2.2. Ion-exchagne textiles

The use of ion-exchange textiles as conductive spacers in the CDI and CEP processes have some advantages compared to ordinary ion-exchange resins (Dejean *et al.* 1997, 1998; Laktionov *et al.* 1999; Dejean 1997; Kourda 2000; Basta *et al.* 1998; Ezzahar *et al.* 1996).

First of all the textile material is much easier to incorporate into an electromembrane cell. The sheet shape nature of the textile makes it convenient to cut a sheet of the desired shape and place it in the dilute compartment, whereas for ion-exchange resins one has to be very careful when placing the resin beads into the compartment as to minimise the risk to create preferential flow channels.

The larger surface to volume ratio of the fibers in the textile ensures a high ion-exchange rate and that a good contact between the membranes and the textile is established.

The ion-exchange textiles gives a lower pressure drop and hence less energy is required to force the flow through the cell. The hydrophilic nature of the fibers and the high porosity of the textiles compared to a resin bed is the reason for the high permeability of the textiles.

CHAPTER 3

Experimental activities

3.1. Iontex

Toxic ionic species removal from drinking and industrial water; new filtration systems using functionalised textiles

The purpose of the EU funded research project Iontex was to develop new functionalised textiles from cellulosic fibers. The six participating companies were;

1. Lenzing, Austria, manufacturer of man-made cellulosic fibres.
2. Institut Francais Textile-Habillement (IFTH), France, textile research institute.
3. Orsa, Italy, manufacturer of non-woven textiles.
4. Protection des Metaux (PM), France, specialists in surface treatment.
5. Eurofiltec, France, manufacturer of filtration equipment.
6. Vattenfall Utveckling AB (VUAB), Sweden, the R&D division of Vattenfall, a swedish utilities company.

In this chapter some of the experimental activities of Vattenfall within the Iontex project will be summarised.

VUAB participated in Iontex as an end user of the developed ion-exchange textile. The task was to develop an electrodialysis module that incorporated ion-exchange textile. The application under consideration was the removal of nitrate form ground water for drinking water production.

In the beginning of the project the following list of desirable textile properties was presented to the other partners in the project.

- The textile should be suitable for drinking water production. No toxic substance should be released to the water. Requirement.
- The textile should have good stability in electric fields. Requirement.
- Mechanical stability at different pH. Desirable.
- A high hydrodynamic permeability allowing for a low pressure drop. Desirable.
- A good electrical conductivity. Desirable.
- A high specific area (area/volume) for improved ion-exchange kinetics. Desirable.
- High ion-exchange capacity. Desirable.
- Affinity for nitrate. Desirable.

Different textile samples was delivered for characterisation at VUAB. Initially the resistance to flow and mechanical stability at different pH, was tested in order to find a textile with suitable properties.

3.1.1. *Permeability tests*

The flow through the textile can be described as a flow through a fibrous porous media governed by Darcy's law.

$$\mathbf{u} = -\frac{\kappa}{\mu}\nabla P \tag{3.1}$$

where κ is the permeability of the textile, μ is the dynamic viscosity of the fluid, $\mathbf{u}$ is the superficial average of the fluid velocity vector and ∇P is the pressure gradient.

The permeability of the textile depends on characteristics of the fibers and on the structure of the fibrous net-work such as the orientation of the fibers. Empirical correlations found in the literature, for fibrous porous media with fibers of circular cross section, reveals that the permeability mainly depends upon two characteristic features of the textile, the porosity and the diameter of the fibers. One example of such a correlation is (Dullien 1992)

$$\kappa = \frac{d_f^2}{64(1-\epsilon)^{3/2}\{1+56(1-\epsilon)^3\}}. \tag{3.2}$$

where d_f is the diameter of the fibers and ϵ is the porosity of the textile.

The permeability of the textile samples was determined by measuring the flow rate as a function of the pressure drop. In figure 3.1 the flow rate versus pressure drop is plotted for three different textile samples. It was found that the textile most suitable for incorporation in the electrodialysis module had a low density, around 100 kg/m^3, and a relatively high permeability, κ=$O(10^{-10})$ m^2.

3.1.2. *Mechanical stability*

The mechanical stability of the textile samples at high pH was poor. Thin textile samples which were left in 1 M NaOH solution for 24 h fell apart into a suspension of fibers. To reduce the problems with mechanical stability in alkaline environment, it was decided to use a textile with a thickness of at least four mm.

3.2. Nitrate removal experiments

Initially two different ion-exchange membrane processes were considered for the removal of nitrate from ground water. The first was CDI and the second was CEP both with the same type of anion-exchange textile incorporated as conducting spacer. Experiments with solutions containing sodium nitrate, sodium chloride and sodium sulphate were conducted with both process configurations. Both recirculated and single pass modes of operation were used and

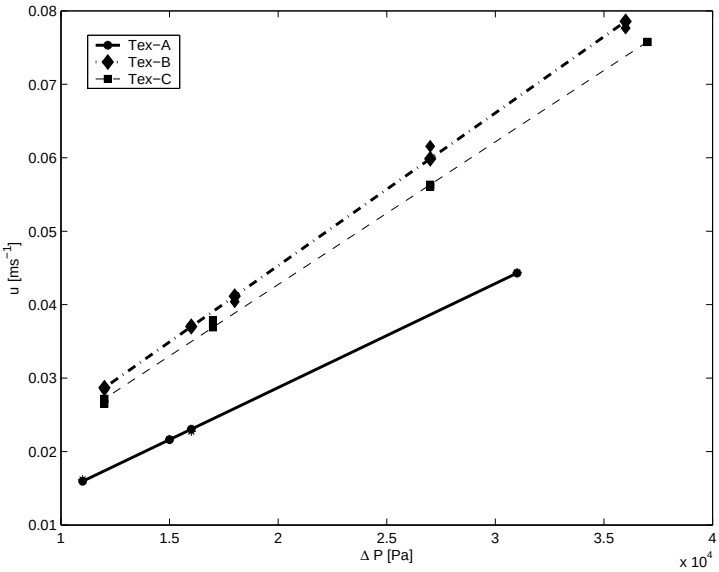

FIGURE 3.1. The flow rate as a function of pressure drop. The slope of the curves are given by $\frac{\kappa}{\mu L}$, where κ is the permeability of the textile, μ is the dynamic viscosity of water and L is the streamwise length of the textile sample. In the figure above $\kappa_A = 2.1 \cdot 10^{-10}\,[\mathrm{m}^2]$, $\kappa_B = 3.1 \cdot 10^{-10}\,[\mathrm{m}^2]$ and $\kappa_C = 2.9 \cdot 10^{-10}\,[\mathrm{m}^2]$

the concentrations of each anion in the product was measured together with the applied current and voltage. A photo of the experimental setup used for these measurements is presented in figure 3.2. From these experiments it was decided to investigate the continuous electropermutation configuration further. The reason for this was the lower power-consumption obtained with this configuration and the preservation of cations which gives a better drinking water quality.

The influence of the developed ion-exchange textile on the CEP process, in a single pass mode of operation, was investigated. This was done by comparing experiment with and without textile incorporated. The results from these experiments are presented in the third paper of the second part of this thesis. Another objective with these experiments were to validate the predictions made by the mathematical model of the CEP process which was developed within the project.

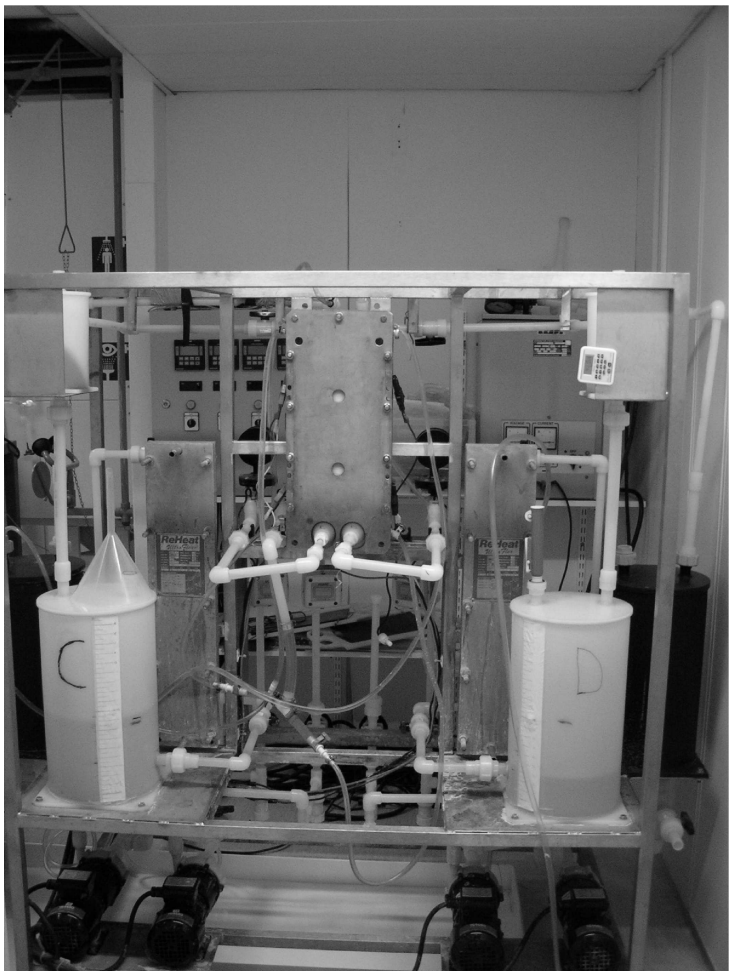

FIGURE 3.2. The experimental setup used to investigate the continuous electropermutation process.

3.3. Evaluation with real groundwater.

Nitrate removal by continuous electropermutation using the Iontex textile was tested on a real groundwater from Sangenhausen region, Germany. In table 3.1 the ionic composition of the Sangenhausen water is presented.

Na^+	NH_4^+	K^+	Cl^-	NO_3^-	SO_4^{2-}
[mg/l]	[mg/l]	[mg/l]	[mg/l]	[mg/l]	[mg/l]
22,8	<0.2	5.4	83.2	77.9	423

TABLE 3.1. Composition of the Sangenhausen water.

Apart from the listed ions the water had very high magnesium and calcium content. The total hardness of the water was 40 German degrees. These cations should not affect the nitrate removal efficiency in the electropermutation configuration. Using the electrodialysis configuration on this water could cause some problems if the pH rises close to the cation exchange membrane. Precipitation of calcium- and magnesium-hydroxide could take place and foul the membrane.

Organic contaminants such as humic acid could also become important factors as many of them are negatively charged which makes them accumulate on the textile and the surface of the membranes. The COD of the water was measured to 5 mg/l.

The ion-exchange textile used was not selective for nitrate. The high levels of competing ions therefore made the efficiency of the nitrate removal with continuous electropermutation rather poor. However, it was possible to reduce the nitrate concentration from 78 ppm to 45 ppm in a single pass operation, with a current density of about 100 A/m^2 and a flow of 0.01 m/s. Using the developed cell this corresponds to a production of 20 l/h per cell. A stack with 50 feed compartments would then be able to treat $1m^3/h$. Using nitrate selective membranes and an ion-exchange textile selective for monovalent ions could increase the efficiency of the process.

The high organic content could cause problems with fouling of the membranes and the ion-exchange bed. When the electropermutation cell was dismantled after the experiments; the first part of the textile was colored dark orange by organic matter present in the water. To investigate the influence of the possible fouling of the textile and membranes further studies should be carried out. It is claimed that the ion-exchange textile is less sensitive to fouling than ordinary ion-exchange resins (Dejean *et al.* 1997). Pretreatment of the water as to remove some of the organic contaminants might be necessary for a successful implementation of the technique.

CHAPTER 4

Modeling

In this chapter a brief introduction to the model presented in the second paper is given. The theory behind the derivation of the macro-homogeneous model equations is presented as well as the constitutive relations needed to obtain a closed system of equations.

The main motivation for developing a mathematical model is to better understand the influence of the different parameters and their interaction on the process. Simulations based on the model would be a valuable tool that could be used to optimise the design of the equipment as well as the operation conditions.

A model of a continuous electropermutation process using ion-exchange textiles was presented by Kourda (2000). This model was a macro-homogeneous model. Ion-exchange equilibrium between the textile and the liquid phase was assumed. Mechanical dispersion was not included and no results from 2-D simulations were presented. The model equations were not analysed and introduced assumptions were not motivated.

The domain included in the model presented in this thesis, is the textile filled feed compartment of an electropermutation cell together with adjacent membranes. The textile is treated as a porous bed consisting of a net-work of solid fibers and the interstitial liquid. The ionic transport can take place in both phases. Equations for conservation of mass are solved in each phase together with the electroneutrality constraint. The membranes are treated as homogeneous solid electrolytes with a homogeneous distribution of fixed charges.

Nernst-Planck's equation is used as the transport equation for all species in both phases of the feed compartment and in the membrane. The flow of water through the textile is a forced flow treated as a plug flow. The convective transport through the membranes is neglected.

The exchange of mass between the phases in the feed compartment takes place via ion-exchange which is assumed to be rate-controlled by the mass transfer on the liquid side of the phase interface. This mass transfer is modeled by a Nernst diffusion layer.

4.1. Volume averaging

To overcome the difficulties associated with the heterogeneous structure of the porous media, the concept of volumetrical averaging is applied. The details of the spatial smoothing process is given by Whitaker (1999).

The superficial averaged concentration of component i in the solution phase is defined as

$$< c >= \frac{\int_{V_\alpha} c \, \mathrm{dV}}{\int_{V_T} \mathrm{dV}} = \frac{1}{V_T} \int_{V_\alpha} c \, \mathrm{dV} \tag{4.1}$$

V_α =Volume of solution phase.
V_T =Total volume.

If one instead averages over the solution volume instead of the total volume the interstitial or intrinsic average of the concentration is obtained.

$$< c >_\alpha = \frac{\int_{V_\alpha} c \, \mathrm{dV}}{\int_{V_\alpha} \mathrm{dV}} \tag{4.2}$$

The interstitial and superficial averages are related through the porosity, ϵ_α,

$$\epsilon_\alpha = \frac{\int_{V_\alpha} \mathrm{dV}}{\int_{V_T} \mathrm{dV}} \tag{4.3}$$

$$< c >= \epsilon_\alpha < c >_\alpha . \tag{4.4}$$

Similar averages are also formed in the textile phase.

4.1.1. *Volume averaged momentum balance.*

The volume average of the Navier-Stokes equations,

$$< \frac{\partial \mathbf{u}}{\partial t} > + < \mathbf{u} \cdot \nabla \mathbf{u} >= - < \frac{1}{\rho} \nabla P > - < \nu \nabla^2 \mathbf{u} >, \tag{4.5}$$

and applying the following assumptions,

- the fluid is Newtonian, and the average momentum transfer via shear stresses is negligible compared to momentum exchange with the solid phase.
- the momentum exchange with the solid phase takes the form of Stokes drag.
- the fluid's inertia has a negligible effect on its momentum balance when compared to momentum losses to the solid phase.

yields Darcy's law, equation 4.6, which is the equation governing flow through porous media.

$$\mathbf{j} = -\frac{\kappa}{\mu} \nabla P \tag{4.6}$$

Where $\mathbf{j}$ is the superficial average of the velocity. κ is the permeability of the textile, μ is the dynamic viscosity. Darcy's equation hold when j is sufficiently small. The Reynolds number, $Re = \frac{j\sqrt{\kappa}}{\nu}$ based on a characteristic length scale of the porous matrix, taken to be the square root of the permeability, should be less than some value between 1 and 10. (Bear 1988).

For our process the typical flow rate is

$$0.01 \leq j \leq 0.1 \qquad [\frac{m}{s}] \tag{4.7}$$

which for a textile with a permeability similar to that developed in the Iontex project corresponds to Reynolds numbers in the range;

$$0.1 \leq Re \leq 1. \tag{4.8}$$

One simplification introduced by the use of Darcy's law is that of neglecting the momentum transfer via shear stresses. This makes it impossible to satisfy the no-slip boundary conditions at the membrane walls. Hence the flow field close to the membranes can not be computed using Darcy's law. The solution to Darcy's law in the bulk of the feed compartment is simply a plug flow. In the model this flow is not calculated. Instead the linear flow velocity is one of the parameters which defines the process conditions.

To satisfy the no-slip condition at the membrane walls an extension to the Darcy's law called the Brinkman equation would have to be used,

$$\nabla P = -\frac{\mu}{\kappa}\mathbf{j} + \mu_{eff}\ \nabla^2\mathbf{j} \tag{4.9}$$

where μ_{eff} is an effective viscosity. A detailed averaging process gives that for an isotropic medium, $\mu_{eff}/\mu = 1/(\epsilon\tau)$, where τ is the tortuosity and ϵ the porosity of the medium (Nield & Bejan 1999). This has however not be considered in the model presented in this thesis.

4.1.2. *Conservation of mass*

Conservation of mass at steady state at the microscopic scale gives,

$$\nabla \cdot \mathbf{N} = 0 \tag{4.10}$$

where $\mathbf{N}$ is the ionic flux. The flux in the presented model is assumed to be governed by Nernst-Planck's equation,

$$\mathbf{N} = \underbrace{-D\nabla c}_{\text{Diffusion}} \underbrace{- zuc\nabla\Phi}_{\text{Migration}} + \underbrace{\mathbf{u}c}_{\text{Convection}} \tag{4.11}$$

The macro-homogeneous version of the mass conservation equations are formulated using superficial averages of the balance equations at the microscopic scale. The steady state version of conservation of mass is written as;

$$< \nabla \cdot \mathbf{N} >= 0 \tag{4.12}$$

Applying the spatial averaging theorem (Whitaker 1999) allows us to express the average of the divergence of the flux as,

$$< \nabla \cdot \mathbf{N} >= \nabla \cdot < \mathbf{N} > + \frac{1}{V}\int_{A_\alpha} \mathbf{N} \cdot \mathbf{n}_\alpha \, \mathrm{dA} \tag{4.13}$$

Where the integral term in equation 4.13 describes the fluxes over the phase interface. The interfacial fluxes enters the macro-homogeneous equations in

the form of sink or source terms. A model for these terms is introduced in the model.

$$S = \frac{1}{V}\int_{A_\alpha} \mathbf{N}\cdot\mathbf{n}_\alpha \,\mathrm{dA} \tag{4.14}$$

Thus the macro-homogeneous version of the equations for conservation of mass is given by,

$$\nabla\cdot <\mathbf{N}> + S = 0. \tag{4.15}$$

There will be one conservation of mass equation in each phase for each specie. Hence, two equations are needed to solve for the distribution of one ionic specie in both phases. Together with the electroneutrality condition this will give a complete set of equations.

The volume averaged flux need to be expressed in terms of the volume averaged concentration and potential. The volume average of the flux is given by,

$$<\mathbf{N}> = - <D\nabla c> - <zuc\nabla\phi> + <\mathbf{u}c>. \tag{4.16}$$

Expressing the concentration as

$$c = <c>_\alpha + c' \tag{4.17a}$$

the potential as

$$\phi = <\phi>_\alpha + \phi' \tag{4.17b}$$

and the velocity as

$$\mathbf{u} = \mathbf{j} + \mathbf{j}' \tag{4.17c}$$

and introducing this into equation 4.16 gives,

$$\begin{aligned} <\mathbf{N}> = & -D\epsilon_\alpha\nabla <c>_\alpha - zu <c>_\alpha \nabla <\phi> + \mathbf{j} <c>_\alpha \\ & - zu <c'\nabla\phi'> + <\mathbf{j}'c'> - zu <c>_\alpha \frac{1}{V}\int_{A_\alpha} \phi\mathbf{n}_\alpha \,\mathrm{dA} \\ & - D\frac{1}{V}\int_{A_\alpha} c\mathbf{n}_\alpha \,\mathrm{dA} \end{aligned} \tag{4.18}$$

The first three terms in the equation above are the obvious candidates for the volume averaged fluxes in all porous material. The rest of the terms describes effects of the inherent structure of the material.

4.1.3. *Effective Diffusivity*

One effect of the heterogeneous structure of the porous media is that the diffusion process will be slower due to the tortuosity of the pores. This is usually modeled by an effective diffusion coefficient, D_e (Bird *et al.* 2002; Newman 1991),

$$D_e = \epsilon_\alpha^{1+b} D \tag{4.19}$$

where ϵ is the porosity and b is a constant normally taken to be 0.5. This will also be used for the migration terms by using the Nernst-Einstein relationship between mobility and diffusivity.

$$u = \frac{F}{RT}D \tag{4.20}$$

where the definition of the ionic mobility, u, given by (Helfferich 1995) is used.

4.1.4. *Mechanical Dispersion*

The term $< \mathbf{j}^{'} c^{'} >$ describes a mixing process known as the mechanical dispersion, its value will depend on both flow field and the geometry. To deal with this term in our model we need to express it in terms of the averaged quantities. The following model is used to incorporate the effects of dispersion (Whitaker 1999),

$$< \mathbf{j}^{'} c^{'} >= -\mathcal{D} \nabla < c >_{\alpha} \tag{4.21}$$

where $\mathcal{D}$ is a tensor which in the case of uniaxial flow along one of the coordinate axes is a diagonal tensor. Note that $\mathcal{D}$ is not an isotropic tensor. Usually the effect of mechanical dispersion is more pronounced in the flow direction. For a uniaxial flow along the y-axis through a isotropic porous material the dispersion tensor would look like,

$$\mathcal{D} = \begin{pmatrix} \mathcal{D}_T & 0 & 0 \\ 0 & \mathcal{D}_L & 0 \\ 0 & 0 & \mathcal{D}_T \end{pmatrix} \tag{4.22}$$

where $\mathcal{D}_L$ is known as the longitudinal coefficient of dispersion and $\mathcal{D}_T$ as the transverse coefficient of dispersion. In the model empirical correlations found in the literature will be used to obtain the values of $\mathcal{D}_L$ and $\mathcal{D}_T$.

4.1.5. *Connectivity*

The fluxes in the two phases of the porous media will in general not be independent of each other.

Basically there are three different routes through the bed by which the ions can be transported.

I) Alternating through the liquid and the solid phase.
II) Only through the solid phase.
III) Only through the liquid phase.

These are illustrated in figure 4.1. The influence of the connectivity of the phases and the path of the ionic fluxes through a bed of ion-exchange material has been discussed several times in the literature (Spiegler *et al.* 1956; Vuoriletho & Tamminen 1997; Yeon *et al.* 2003; Yeon & Moon 2003). In a model of the heterogeneous structure of some ion-exchange membranes by Zabolotsky & Nikonenko (1993), two extreme cases for the arrangement of the ion-exchange phase and the liquid phase are discussed. The two phases are either arranged in parallel to each other or in a serial arrangement as is shown in figure 4.2. The actual arrangement can be described as some combination of these two. In the model presented in this thesis only the parallel arrangement is considered. A future improvement of the model would be to incorporate the porous plug model (Spiegler *et al.* 1956) to include effects of the connectivity of the material.

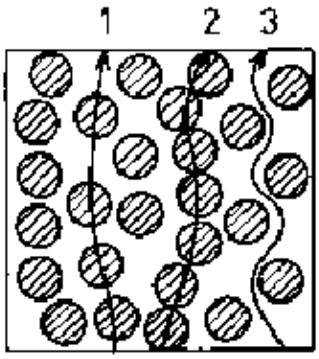

FIGURE 4.1. Schematic of the charge transport through a bed of solid ion-exchange material and liquid electrolyte (Spiegler *et al.* 1956).

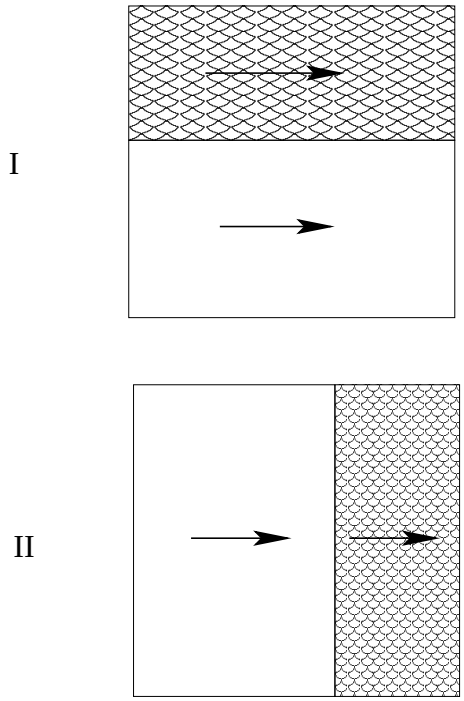

FIGURE 4.2. The two extreme cases of all possible paths for the ionic fluxes. I) Parallel arrangement of the two phases. II) Serial arrangement of the phases. Introduced by (Spiegler *et al.* 1956).

CHAPTER 5

Summary

A summary of the results presented in the second part of this thesis is given in this chapter.

In the first paper the design of a new frame for the ElectroSynCell ,to be used together with the Iontex textiles, is described. Three different frame designs were proposed. The flow field through them were calculated using two different 2-D models of the momentum equations. The calculated flow distributions, without textile incorporated, suggested that a sophisticated flow distribution design was not needed. The relatively narrow compartment provided a high resistance to the flow leading to a fair flow distributions with all proposed frame designs.

A simplified version of one of the proposed frame designs was chosen and a prototype was manufactured. In figure 5.1 a photo of the prototype frame is shown. In the photo a piece of ion-exchange textile is incorporated. A photo from the flow visualisation experiments conducted is presented in figure 5.2. A red tracer color is injected and the distribution of the color gives an indication of the uniformity of the flow field.

The main result of the modeling activities presented in the second paper is the identification of the three governing dimensional numbers presented below.

The first of these numbers is,

$$\Delta = \frac{2D^m c_0^m}{\mu\sigma j_0 c_0}, \tag{5.1}$$

which gives an indication of the importance of the removal by Donnan dialysis. D^m is the diffusivity in the membrane, c_0^m is the concentration of fixed charges in the membrane, μ is the thickness of the membranes, j_0 is the superficial average of the fluid velocity and c_0 is a typical concentration of nitrate in the solution. A high value of Δ indicates that no electric current need to be applied. The nitrate removal can then be achieved via Donnan dialysis; by a suitable choice of the composition of the concentrate solution.

The second dimensionless number is,

$$\chi = \frac{\mathcal{V}}{\sigma^2 Pe}. \tag{5.2}$$

Where $\mathcal{V} = \frac{F\phi_0}{RT}$, $\sigma = \frac{h}{L}$ and $Pe = \frac{j_0 L}{D_0}$. L is the streamwise length and h is the thickness of the feed compartment. ϕ_0 is the potential drop over the feed

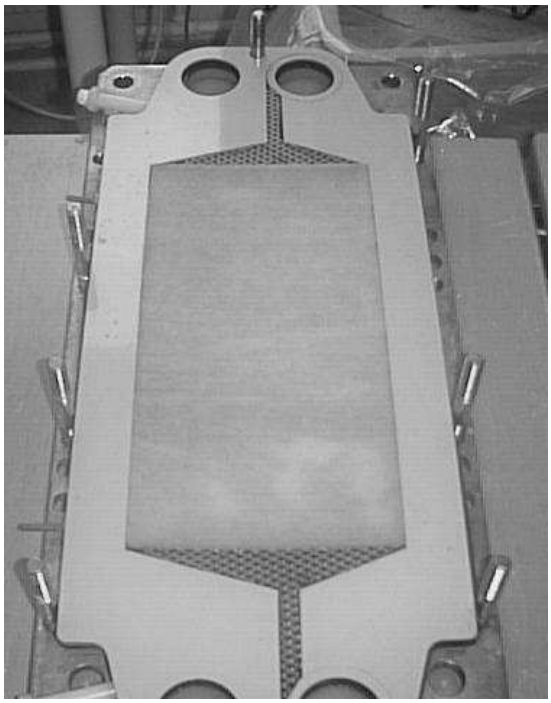

FIGURE 5.1. Photo of the developed frame. An ion-exchange textile is incorporated as spacer and net-type spacers are placed in the inlet and outlet sections.

compartment and adjacent membranes. j_0 is the linear velocity of the flow. D_0 is a typical diffusivity of the ions in water. The optimal process conditions, for a fixed equipment design, can be found by doing a parametric study of the influence of χ. In figure 5.3 the concentration of nitrate in the product as a function of χ is presented for different values of Δ. Since the potential drop over the feed compartment enters rather than the current density, this dimensionless number is independent of the concentration of the feed solution.

The third dimensionless number highlighted in the modeling paper is,

$$Z = \frac{w\rho_\beta}{\epsilon_\beta c_0}. \tag{5.3}$$

This is the ratio between the intrinsic averages of the concentrations in the textile and the solution. w is the capacity of the textile, ρ_β is the density of the textile, ϵ_β is the volume fraction of the textile phase and c_0 is the concentration of nitrate in the solution.

Other important results presented in the modeling paper are related to the analysis of the model equations. The following assumptions used in the model presented by Kourda (2000) are identified and motivated.

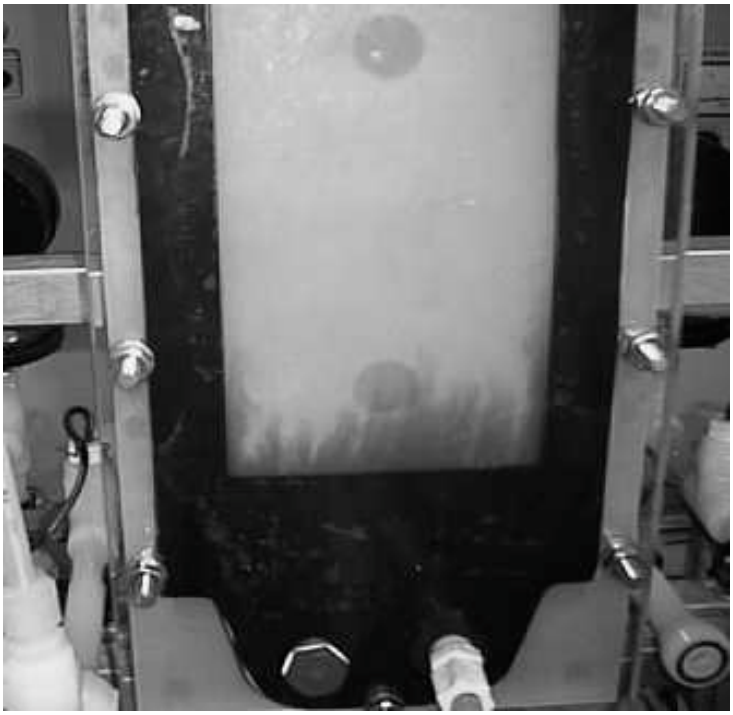

FIGURE 5.2. A photo from the flow visualisation experiments conducted with the developed frame design. No ion-exchange textile is incorporated. A spacer net is used in the inlet and outlet section according to figure 5.1

- The long and slender geometry of the feed compartment makes it possible to reduce the fully elliptic problem to a parabolic problem.
- The large specific surface area of the textile ion-exchanger motivates the assumption that ion-exchange equilibrium prevail between the phases. This reduces the model to a one-equation model.

In the third paper the continuous electropermutation process is investigated experimentally. The frame design described in the first paper was used in the experiments. The influence of the textile was shown by comparing experiments with and without the ion-exchange textile incorporated. From an initial nitrate concentration of 105 ppm it was possible to obtain a product stream with only 15 ppm nitrate. The linear flow velocity through the feed compartment was 1.2 cm/s corresponding to a flow rate of 20 l/h per elementary cell.

It was also found that the pressure drop over the different compartments influences the performance of the process significantly. If the pressure drop over the concentrate compartment is too low, preferential flow paths are created in between the membrane and the textile in the feed compartment. This was

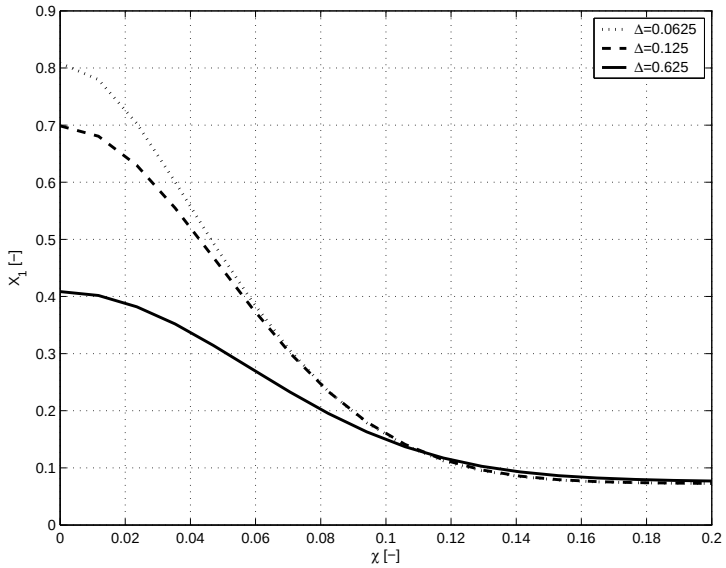

FIGURE 5.3. The concentration of nitrate at the outlet as a function of χ obtained from simulations of continuous electropermutation. The different curves represent different values of the dimensionless number Δ as indicated in the figure. The value of Z in these simulation was 620.

supported by the similar results obtained with and without textile incorporated. Furthermore, the parts of the textile which were in contact with the water was colored by organic compounds present in the water. The location of the colored areas on the textile confirmed that the liquid bypassed the textile. The conclusions drawn from this is that a good mechanical support for the membrane is needed to ensure that sufficient contact is established between the membrane and the ion-exchange textile. One way to minimise these problems would be to incorporate ion-exchange textiles in both the concentrate and the feed compartment. This would make it easier to control the pressure difference over the membrane.

The experimental results were compared to the model predictions, as can be seen in figure 5.4 a good agreement between the model and the experiments was obtained. There are several model parameters in the model which are unknown at the moment; however, all model parameters can be determined individually in experiments where one can isolate their influence.

5.1. Outlook

The effect of the heterogeneous structure of the textile should be incorporated in the model. This would make it possible to compare the behavior of different spacer materials using the model.

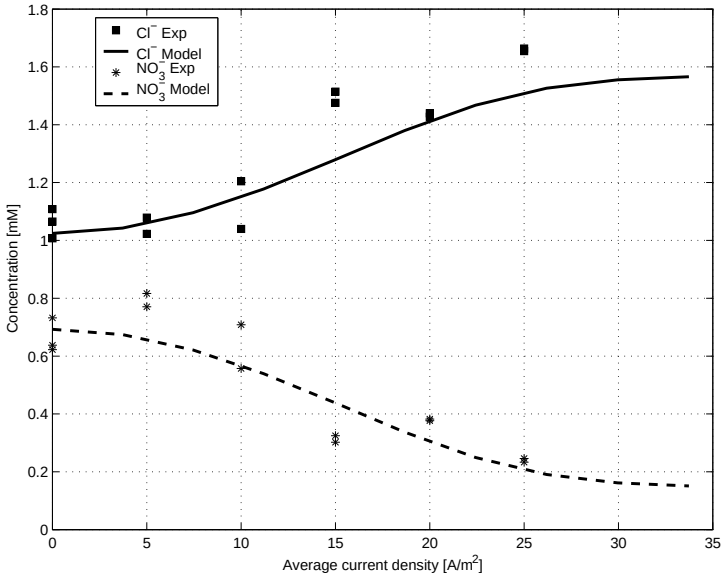

FIGURE 5.4. The model predictions for the outlet concentrations of chloride and nitrate plotted against the average current density together with the experimental results.

The influence of water splitting taking place at the membrane interface could be included in the model by resolving the boundary layer close to the wall. The process can then be simulated at higher current densities allowing for higher flow rates or thicker compartments.

Modifying the model as to be able to simulate electrodeionisation would be an interesting step to take. The influence of different options to compose the ion-exchanger used as conducting spacer could then be studied with the model.

One of the main advantages of the newly developed ion-exchange textile is the high specific surface area. This gives very fast ion-exchange kinetics, making it ideal for removal of impurities present in very low concentrations. The concentration of low grade active waste solutions in the nuclear industry is one possible application where this might be of use. Other applications is related to the removal of very low levels of heavy metals in the production of drinking water.

Acknowledgment

This work was financed by the VINNOVA competence center, FaxénLaboratoriet, with the main industrial partner in this project being Vattenfall AB.

I would like to thank my supervisors Docent Anders Dahlkild, Dr. Anna Velin and Dr. Mårten Behm for giving me the opportunity work on this project and for all the valuable feedback they have given me from the beginning of this project.

The Iontex partners are greatly acknowledged. I want to thank for all the interesting and rewarding meetings.

I want to thank all my colleagues at the department for providing a good working atmosphere and interesting discussion during the coffee breaks. My room mates over the years, Dr. Erik Birgersson, Dr. Karl Borg, Dr. Henrik Sandqvist, Niklas Mellgren, Dr. Martin Skote, Olivier Macchion and Mattias Jansson I have learnt a lot from you for which I am very grateful.

The time spent in VUAB's electrochemistry lab would not been as enjoyable without the people working there. I wish to thank; Bosse, thanks for helping me with the analysis and for all the interesting food which made the lunches at the lab ever so interesting. Anna, Noemi, Jinjin, Anders Wårlin, Stefan Velin, Anders Wiik and Leif Liinankii.

Prof. Fritz Bark and Dr. Rolf Karlsson are acknowledged for their interest in my work and for their work within the Faxen laboratory. Dr. Ann Cornell, Prof. Göran Lindberg and the others in Electrochemistry group within FaxenLaboratoriet. Our meetings always give new inspiration.

I would also like to thank all of my friends and family for their love and support.

Last but not least. Elin, thank you for all your love and support. Jag Älskar dig!

Nomenclature

	Description
Roman letters	
c	concentration [mol/m^3]
d_f	Fibre diameter [m]
D	Diffusion coefficient [m^2/s]
$\mathcal{D}$	Mechanical dispersion tensor [m^2/s]
$\mathcal{D}_{\mathcal{L}}$	Coefficient of transversal dispersion [m^2/s]
$\mathcal{D}_{\mathcal{T}}$	dispersion tensor [m^2/s]
F	Faraday's constant F = 96485 [C/mol]
h	Thickness of feed compartment [m]
j	Superficial velocity [m/s]
L	Length of feed compartment [m]
N	Ionic flux [mol/(m^{2}s)]
R	Gas constant R=8.3145 [J/(mol K)]
P	Pressure [Pa]
S	Sink/source term from ion-exchange rate [mol/(m^{3}s)]
T	Temperature [K]
u	Velocity vector [m/s]
u	Ionic mobility [m^{2}mol/(Js)
$\mathcal{V}$	Non dimensional potential scale $\frac{F\phi_0}{RT}$[-]
z	Valence of ion [-]
Z	Ratio between the intrinsic concentration scales in both phases $\frac{w\rho_\beta}{\epsilon c_0}$ [-]
Greek letters	
χ	Non dimensional number defined as $\frac{\mathcal{V}}{\sigma^2 Pe}$ [-]
Δ	Non dimensional number $\frac{2D^m c_0^m}{\mu\sigma j_0 c_0}$ [-]
ϵ	Volume fraction [-]
κ	Permeability [m^2]
μ	Dynamic viscosity [Pas]
μ	Thickness of membrane [m]
ν	Kinematic viscosity [m^2/s]
ω	concentration of fixed charges in the solid phase [mol/m^3]
ϕ	potential [V]
ρ	Density [kg/m^3]
σ	Ratio of thickness to length of feed compartment, $\frac{h}{L}$[-]
τ	Tortuosity [-]
Symbols	
$< .. >$	Superficial volume average
$< .. >_\alpha$	Intrinsic volume average of α-phase.
$< .. >_\beta$	Intrinsic volume average of β-phase.

Subscript	
α	Refers to liquid-phase
β	Refers to textile-phase
i	Specie i
Superscript	
'	Deviation from volume average
m	Refers to membrane

Bibliography

Basta, K., Aliane, A., Lounis, A., Sandeaux, R., Sandeaux, J. & Gavach, C. 1998 Electroextraction of Pb^2+ ions from diluted solutions by a process combining ion-exchange textiles and membranes. *Desalination* **120**, 175–184.

Bear, J. 1988 *Dynamics of Fluids in Porous Media*. Dover, iSBN 0-486-65675-6.

Bird, R., Stewart, W. & Lightfoot, E. 2002 *Transport Phenomena*, 2nd edn. Wiley.

Dejean, E. 1997 Electrodesionisation sur textiles echangeurs d'ions. PhD thesis, Universitet Montpellier II.

Dejean, E., Laktionov, E., Sandeaux, J., Sandeaux, R., Pourcelly, G. & Gavach, C. 1997 Electrodeionization with ion-exchange textile for the production pf high resistivity water: Influence of the nature of the textile. *Desalination* **114**, 165–173.

Dejean, E., Sandeaux, J., Sandeaux, R. & Gavach, C. 1998 Water demineralization by electrodeionization with ion-exchange textiles. comparison with conventional electrodialysis. *Separation Science and Technology* **33** (6), 801–818.

Dullien, F. 1992 *Porous Media, Fluid Transport and Pore Structure*, 2nd edn. Academic Press.

European Community 1998 Council directive of 3 november 1998. Official J.Europ.Commun., L330, 05/12/1998 P. 0032 - 0054.

Ezzahar, S., Cherif, A., Sandeaux, J., Sandeaux, R. & Gavach, C. 1996 Continuous electropermutation with ion-exchange textiles. *Desalination* **104**, 227–233.

Helfferich, F. 1995 *Ion Exchange*. Dover, iSBN 0-486-68784-8.

Hult, A. 1998 Dricksvattensituationen i sverige. *Tech. Rep.*. VAV AB, 91-89182-11-1.

Kapoor, A. & Viraraghavan, T. 1997 Nitrate removal from drinking water - review. *Journal of Environmental Engineering* pp. 371–380.

Kesore, K., Janowski, F. & Shaposhnik, V. 1997 Highly effective electrodialysis for selective elimination of nitrates from drinking water. *Desalination* **127**, 17–24.

Kourda, N. 2000 Électropermutation sur textiles Échangeurs de cations. PhD thesis, Universitet Montpellier II.

Laktionov, E., Dejean, E., Sandeaux, J., Gavach, C. & Pourcelly, G. 1999 Production of high resistivity water by electrodialysis. influence of ion-exchange textiles as conducting spacers. *Separation Science and Technology* **34**, 69–84.

Mulder, M. 1996 *Basic Principles of Membrane Technology*. Kluwer Academic Publishers.

Newman, J. S. 1991 *Electrochemical Systems*, 2nd edn. Prentice Hall, iSBN: 0-13-248758-6.

Nield, D. & Bejan, A. 1999 *Convection in Porous Media*. Springer, iSBN 0-387-98443-7.

Salem, K., Sandeaux, J., Molénat, J., Sandeaux, R. & Gavach, C. 1995 Elimination of nitrate from drinking water by electrochemical membrane processes. *Desalination* **101**, 123–131.

Schoebesberger, H., Einzmann, M., Schmidtbauer, J., Gayrine, P. & Martinetti, R. 2004 Iontex-viscose fibers with ion exchange properties. *Chemical Fibes International* **54** (2), 101–111.

Schoeman, J. & Steyn, A. 2003 Nitrate removal with reverse osmosis in a rural area in south africa. *Desalination* **155** (1), 15–26.

Spiegler, K., Yoest, R. & Wyllie, M. 1956 Electrical potentials across porous plugs and membranes, ion-exchange resin-solution systems. *Disc.Faraday.Soc.* **21**, 174.

Vuoriletho, K. & Tamminen, A. 1997 Application of a solid ion-exchange electrolyte in three-dimensinal electrodes. *Journal of Applied Electrochemistry* **27**, 749–755.

Whitaker, S. 1999 *The Method of Volume Averaging*. Kluwer Academic Publisher, iSBN 0-7923-5486-9.

WHO 2004 Guidlines for drinking water quality; recomendations i, geneva. 3rd Edition.

Yeon, K. & Moon, S. 2003 A study on removal of cobalt from primary coolant by continuous electrodeionization with various conducting spacers. *Separation Science and Technology* **38** (10), 2347–2371.

Yeon, K., Seong, J., Rengaraj, S. & Moon, S. 2003 Electrochemical characterization of ion-exchange resin beds and removal of cobalt by electrodeionization for high-purity water production. *Separation Science and Technology* **38** (2), 443–462.

Zabolotsky, V. & Nikonenko, V. 1993 Effect of structural membrane inhomogeneity on transport properties. *Journal of Membrane Science* **79**, 181–198.

1

Paper 1

Flow Distribution Study of a New Electrodialysis Module.

By Carl-Ola Danielsson[1], Anna Velin[2], Anders Dahlkild[1] & Mårten Behm[3]

The purpose of this project was to develop a membrane module that could be used for ion-exchange assisted electrodialysis, using four mm thick ion-exchange textiles as conducting media. The proposed design is based on the ElectroSynCell. New frames which enables the use of four mm thick compartments have been developed. The flow field through different proposed frame design was conducted and after this a prototype was manufactured and the flow field obtained was tested experimentally.

1. Introduction

The aim of the EU funded research project Iontex was to develop new functionalised textiles made out of cellulosic fibers, for filtration applications (Schoebesberger *et al.* 2004). This report describes the development of a specific electrodialysis module, which could incorporate ion-exchange textile in an electro membrane process, which was Vattenfall Utveckling AB's (VUAB) task in the Iontex project. The specific application in mind was removal of nitrate from groundwater to produce drinking water.

In the beginning of the project the type of textile to be used together with the developed equipment was chosen. Different types of non-woven textiles without the ion-exchange functionality incorporated were evaluated in terms of hydrodynamic permeability and mechanical strength. It was found that the textile to be used needed a low density, around 100 kg/m^3, to provide a relatively high permeability, $\kappa = O(10^{-10})\mathrm{m}^2$. A thickness of four mm was required to provide a sufficient mechanical stability. This characterisation of the textiles gave the input parameters needed for the design of the ED module. The thickness of the compartments was to be four mm. Using one mm thick EPDM gaskets on each side of the frames left us with two mm thick frames to design.

It was decided that the design of the ED module should be based on the ElectroSynCell® which has been described in detail in the literature (Bengoa

[1]Department of Mechanics, KTH, SE-100 44 Stockholm, Sweden.
[2]Vattenfall Utveckling AB, SE-100 00 Stockholm, Sweden.
[3]Department of Chemical Engineering and Technology, KTH, SE-100 44 Stockholm, Sweden.

et al. 1997; Carlsson *et al.* 1982, 1983). New thinner frames had to be developed in order to incorporate the textile. The new frames should be designed as to provide as uniform flow distributions as possible. Computer simulation of the flow distribution was conducted to compare the flow distributions provided by different proposed frame designs. In all calculations of the flow distributions it was assumed that the textile was not incorporated. Incorporation of the textile would result in a even more uniform flow distribution.

Studies of the fluid mechanics of filter-press type reactors in the literature include work on heat exchangers, electrodialysis cells, reverse osmosis units and other pressurised membrane techniques (Belfort 1972; Pellegrin *et al.* 1995; Karode & Kumar 2001; Cao *et al.* 2001). The majority of these publications have focused on the mass/heat transfer and the effects of spacers as turbulence promoters.Bengoa *et al.* (1997) made a study of the residence time distribution, which is a measure of the flow pattern inside the cell, using the ElectroSynCell® they also made similar studies of the FM01-LC cell (Bengoa *et al.* 2000).

Only a few publications have been found were the flow distribution design has been in focus. Darcovich *et al.* (1997) designed a membrane module with uniform flow distribution in order to test be able to compare different membranes. The inlet section of this membrane module was allowed to be long compared to the active area as to ensure as uniform flow as possible. In our case it is desired to have an as shot inlet section and outlet section as possible to maximise the active area of the module. Kho & Muller-Steinhagen (1999) highlighted the effects of flow distribution in parallel plate heat exchangers and the effect it has on corrugation patterns. They also compared five different flow distributor designs. The geometry of the heat exchangers is very similar to that of the electrodialysis module. However, the linear flow velocities through the heat exchangers were more than one order of magnitude higher than what is expected through the electrodialysis module.

2. Theoretical flow field studies

The three proposed frame designs shown in figure 1 were investigated. Design A (to the left) has channels to distribute the flow over the width of the active area of the module. This design has several different design parameters such as the number of channels and the width of each channel. The idea behind design B (in the center) is to use a porous material in front of the active area. A major advantage of this design compared to the other two is that it is easy to manufacture. The ion-exchange textile itself could be used as flow distributor by letting the textile be a little bit bigger than the active area of the module. In the flow distribution study design B was split into design B1 and B2. B1 had no porous distributor and B2 had a porous distributor with a permeability comparable to that of the ion-exchange textile. Frame design C (to the right) was similar to the original ElectroSynCell® flow distribution system.

The flow field through the cell was to be calculated using a CFD software. Rather then solving a full 3-D problem for the whole module a simplified 2D model was applied which could be solved using Femlab with less computational effort.

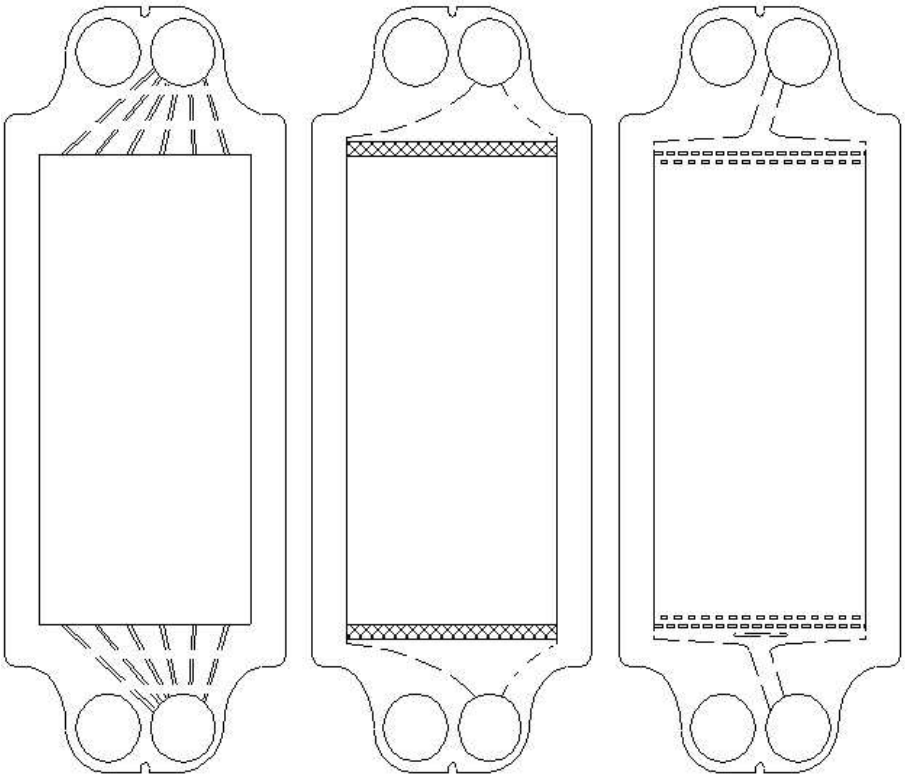

FIGURE 1. The proposed designs of the new frames for the ElectroSynCell®. Design A to the left, B in the center and C to the right.

2.1. *Governing equations*

The governing equations for the velocity field, $\mathbf{u} = (u, v, w)$, and the pressure, P, are the equations for continuity of mass and momentum. Navier-Stokes equations

$$\rho(\frac{\partial \mathbf{u}}{\partial t} + \mathbf{u} \cdot \nabla \mathbf{u}) = -\nabla P + \mu \nabla^2 \mathbf{u} \tag{1}$$

$$\frac{\partial \rho}{\partial t} + \nabla \cdot \rho \mathbf{u} = 0 \tag{2}$$

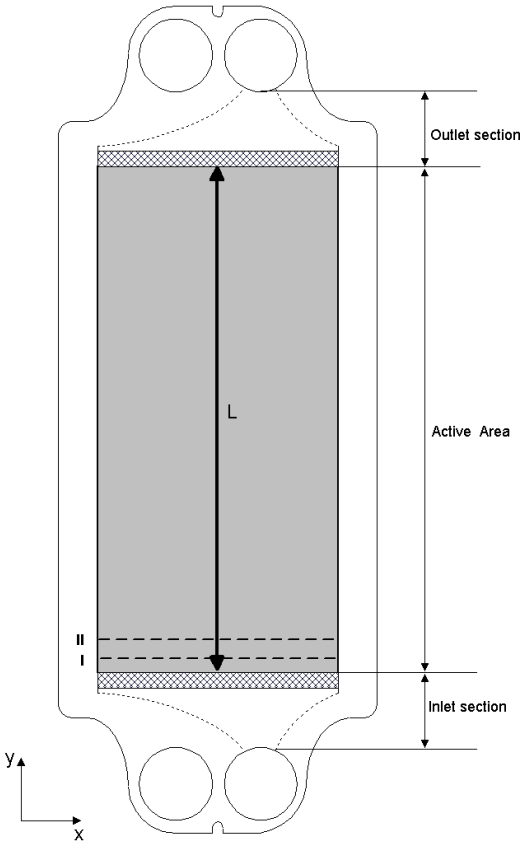

FIGURE 2. The three parts of the frame is the inlet region, the active area and the outlet region. The inlet region distributes the flow and provides a uniform flow distribution before the active area. The active area, grey area in the figure, is where the ionic transport over the membranes take place in an electrodialysis module. Finally in the outlet region the fluid is collected into the outlet stream. The length scale used to scale the equations is the length of the active area, L. The height of the flow compartment in the z-direction, perpendicular to the figure, h is small so that $\sigma = \frac{h}{L}$ is small

The equations are made non-dimensional by introducing the following variables,

$$\begin{aligned} \tilde{x} = \frac{x}{L},\ \tilde{y} = \frac{y}{L},\ \tilde{z} = \frac{z}{\sigma L}, \\ \tilde{u} = \frac{u}{u_0},\ \tilde{v} = \frac{v}{u_0},\ \tilde{w} = \frac{w}{\sigma u_0},\ \tilde{P} = \frac{P}{\rho u_0^2} \end{aligned} \tag{3}$$

where $\sigma = \frac{h}{L}$ is a small dimensionless parameter for a long and slender geometry. The length scale L here is the length of the active area and h is half the height of the flow channel.

Inserting these non-dimensional variables into the steady state form of the Navier-Stokes equations yields

$$\tilde{u}\frac{\partial \tilde{u}}{\partial \tilde{x}} + \tilde{v}\frac{\partial \tilde{u}}{\partial \tilde{y}} + \tilde{w}\frac{\partial \tilde{u}}{\partial \tilde{z}} = -\frac{\partial \tilde{P}}{\partial \tilde{x}} + \frac{1}{Re}(\frac{\partial^2 \tilde{u}}{\partial \tilde{x}^2} + \frac{\partial^2 \tilde{u}}{\partial \tilde{y}^2} + \frac{1}{\sigma^2}\frac{\partial^2 \tilde{u}}{\partial \tilde{z}^2}) \tag{4a}$$

$$\tilde{u}\frac{\partial \tilde{v}}{\partial \tilde{x}} + \tilde{v}\frac{\partial \tilde{v}}{\partial \tilde{y}} + \tilde{w}\frac{\partial \tilde{v}}{\partial \tilde{z}} = -\frac{\partial \tilde{P}}{\partial \tilde{y}} + \frac{1}{Re}(\frac{\partial^2 \tilde{v}}{\partial \tilde{x}^2} + \frac{\partial^2 \tilde{v}}{\partial \tilde{y}^2} + \frac{1}{\sigma^2}\frac{\partial^2 \tilde{v}}{\partial \tilde{z}^2}) \tag{4b}$$

$$\tilde{u}\frac{\partial \tilde{w}}{\partial \tilde{x}} + \tilde{v}\frac{\partial \tilde{w}}{\partial \tilde{y}} + \tilde{w}\frac{\partial \tilde{w}}{\partial \tilde{z}} = -\frac{1}{\sigma^2}\frac{\partial \tilde{P}}{\partial \tilde{z}} + \frac{1}{Re}(\frac{\partial^2 \tilde{w}}{\partial \tilde{x}^2} + \frac{\partial^2 \tilde{w}}{\partial \tilde{y}^2} + \frac{1}{\sigma^2}\frac{\partial^2 \tilde{w}}{\partial \tilde{z}^2}) \tag{4c}$$

where, $Re = \frac{\rho u_o L}{\mu}$ is the Reynolds number.

The conservation of mass equation for an incompressible fluid gives,

$$\frac{\partial \tilde{u}}{\partial \tilde{x}} + \frac{\partial \tilde{v}}{\partial \tilde{y}} + \frac{\partial \tilde{w}}{\partial \tilde{z}} = 0 \tag{5}$$

2.2. *Boundary Conditions*

The boundary conditions that applies to these equations are no-slip at all solid boundaries. A prescribed inlet velocity and the relative pressure set to zero at the outlet boundary.

2.3. *Thin film flow approximation*

The inertia term $(\mathbf{u} \cdot \nabla)\mathbf{u}$, on the left hand side of the momentum balances above can be neglected in comparison to the friction forces at the walls of the channel if (Acheson 1990),

$$\frac{u_0 L}{\nu}\left(\frac{h}{L}\right)^2 \ll 1. \tag{6}$$

where ν is the kinematic viscosity of the fluid.

The following characteristic values for the flow through the electrodialysis module;

$$L = 0.3 \text{ m},\ \mathrm{u}_0 = 0.01 \text{ m/s},\ \mathrm{h} = 0.002 \text{ m} \tag{7}$$

gives,

$$\frac{u_0 L}{\nu}\left(\frac{h}{L}\right)^2 \approx 0.1. \tag{8}$$

The characteristic values above are taken from the active area of the electrodialysis module. Hence, the flow field can to a first approximation be obtained by solving the equations given by the thin film theory (Acheson 1990);

$$\frac{\partial \tilde{P}}{\partial \tilde{x}} = \frac{1}{Re}\frac{1}{\sigma^2}\frac{\partial^2 \tilde{u}}{\partial \tilde{z}^2} \tag{9a}$$

$$\frac{\partial \tilde{P}}{\partial \tilde{y}} = \frac{1}{Re}\frac{1}{\sigma^2}\frac{\partial^2 \tilde{v}}{\partial \tilde{z}^2} \tag{9b}$$

$$\frac{\partial \tilde{u}}{\partial \tilde{x}} + \frac{\partial \tilde{v}}{\partial \tilde{y}} = 0 \tag{9c}$$

Assuming that the u and v velocities can be approximated by fully developed Poiseuille profiles between the membranes gives that

$$u = U_{CL}(x,y)(1 - \frac{z^2}{h^2}) \tag{10a}$$

$$v = V_{CL}(x,y)(1 - \frac{z^2}{h^2}) \tag{10b}$$

where U_{CL} and V_{CL} are the centerline velocities. Thus the equations given by the thin film theory in dimensional form reduces to

$$\frac{\partial P}{\partial x} = -\frac{2\mu}{h^2}U_{CL}(x,y) \tag{11a}$$

$$\frac{\partial P}{\partial y} = -\frac{2\mu}{h^2}V_{CL}(x,y) \tag{11b}$$

$$\frac{\partial U_{CL}(x,y)}{\partial x} + \frac{\partial V_{CL}(x,y)}{\partial y} = 0 \tag{11c}$$

Which can be further simplified,

$$\frac{\partial^2 P}{\partial x^2} + \frac{\partial^2 P}{\partial y^2} = 0, \tag{12}$$

which is a Laplace equation for the pressure,

$$\nabla^2 P = 0. \tag{13}$$

This equation was solved using the commercial finite element code Femlab. The following boundary conditions were imposed;

$$-\frac{h^2}{2\mu}\nabla P = \mathbf{U}_{CL0} \quad \text{at inlet boundary,} \tag{14a}$$

$$P = 0 \quad \text{at outlet boundary,} \tag{14b}$$

$$\mathbf{n}\cdot\nabla P = 0 \quad \text{at solid boundaries.} \tag{14c}$$

where $\mathbf{U}_{CL0} = (U_{CL0}, V_{CL0})$ is the prescribed inlet velocity.

The velocity used in the scaling of the equations leading to the thin film approximation, was the linear flow velocity of the liquid in the active area of the module. In the inlet and outlet sections of the cell the velocities of the liquid is about one order of magnitude higher, furthermore the length of these regions is about one order of magnitude lower. Using the thin film approximation in this region might be a bit optimistic. Therefor an alternative formulation of the 2-D momentum balance equations were also considered.

2.4. *Averaged Navier-Stokes equations*

Averaged equations for the flow distribution in the X-Y plane are obtained by integrating the equations for the u and v velocities over the gap between the membranes.

The Navier-Stokes equations are integrated over channel height from $z = -h$ to $z = h$.

$$\int_{-h}^{h} u\frac{\partial u}{\partial x} + v\frac{\partial u}{\partial y}\mathrm{d}z = \int_{-h}^{h} -\frac{\partial P}{\partial x} + \mu(\frac{\partial^2 u}{\partial x^2} + \frac{\partial^2 u}{\partial y^2} + \frac{\partial^2 u}{\partial z^2})\,\mathrm{d}z \tag{15a}$$

$$\int_{-h}^{h} u\frac{\partial v}{\partial x} + v\frac{\partial v}{\partial y}\mathrm{d}z = \int_{-h}^{h} -\frac{\partial P}{\partial y} + \mu(\frac{\partial^2 v}{\partial x^2} + \frac{\partial^2 v}{\partial y^2} + +\frac{\partial^2 v}{\partial z^2})\mathrm{d}z \tag{15b}$$

The terms,

$$\frac{\partial^2 u}{\partial z^2} \quad \text{and} \quad \frac{\partial^2 v}{\partial z^2},$$

have to be evaluated. Making use of the assumptions of developed Poiseuille profiles once again and performing the integrations gives the following equations,

$$\frac{8}{15}\rho(U_{CL}\frac{\partial U_{CL}}{\partial x} + V_{CL}\frac{\partial U_{CL}}{\partial y}) = -\frac{\partial P}{\partial x} + \frac{2}{3}\mu(\frac{\partial^2 U_{CL}}{\partial x^2} + \frac{\partial^2 U_{CL}}{\partial y^2}) - \frac{2\mu U_{CL}}{h^2} \tag{16a}$$

$$\frac{8}{15}\rho(U_{CL}\frac{\partial V_{CL}}{\partial x} + V_{CL}\frac{\partial V_{CL}}{\partial y}) = -\frac{\partial P}{\partial y} + \frac{2}{3}\mu(\frac{\partial^2 V_{CL}}{\partial x^2} + \frac{\partial^2 V_{CL}}{\partial y^2}) - \frac{2\mu V_{CL}}{h^2} \tag{16b}$$

From this an effective viscosity, μ_{eff} and density, ρ_{eff} can be identified.

$$\mu_{eff} = \frac{2}{3}\mu, \quad \rho_{eff} = \frac{8}{15}\rho$$

The last terms are included in the 2-D averaged version of the momentum balance equations as body forces,

$$\rho_{eff}(U_{CL}\frac{\partial U_{CL}}{\partial x} + V_{CL}\frac{\partial U_{CL}}{\partial y}) = -\frac{\partial P}{\partial x} + \mu_{eff}(\frac{\partial^2 U_{CL}}{\partial x^2} + \frac{\partial^2 U_{CL}}{\partial y^2}) + F_x \tag{17a}$$

$$\rho_{eff}(U_{CL}\frac{\partial V_{CL}}{\partial x} + V_{CL}\frac{\partial V_{CL}}{\partial y}) = -\frac{\partial P}{\partial y} + \mu_{eff}(\frac{\partial^2 V_{CL}}{\partial x^2} + \frac{\partial^2 V_{CL}}{\partial y^2}) + F_y \tag{17b}$$

where

$$F_x = -\frac{2\mu}{h^2}U_{CL}(x,y), \quad F_y = -\frac{2\mu}{h^2}V_{CL}(x,y)$$

This form of the equations were solved using Femlab. The solution gives U_{CL} and V_{CL} which are the centerline velocity in the x and y direction respectively.

The prescribed boundary conditions when solving the averaged Navier-Stokes equations are;

$$\mathbf{U}_{CL} = \mathbf{U}_{CL0} \quad \text{at inlet boundary,} \tag{18a}$$

$$P = 0 \quad \text{at outlet boundary,} \tag{18b}$$

$$\mathbf{U}_{CL} = 0 \quad \text{at wall boundaries.} \tag{18c}$$

Both the averaged equations and TFT equations were derived assuming an empty channel. Introducing a spacer in the channel gives additional resistance to the flow which could be modeled using body forces which are functions of the fluid velocity.

2.5. *Femlab*

The incompressible Navier-Stokes mode of Femlab was used to solve the averaged Navier-Stokes equations and the Darcy flow mode was used for the TFT equations. In Femlab's graphical user interface the geometry of the different frames were defined. Then the appropriate boundary conditions and equation parameters where specified. The equations where solved on a coarse mesh which was gradually refined until mesh independent solutions were obtained. In figure 3 the geometries and the meshes used are shown.

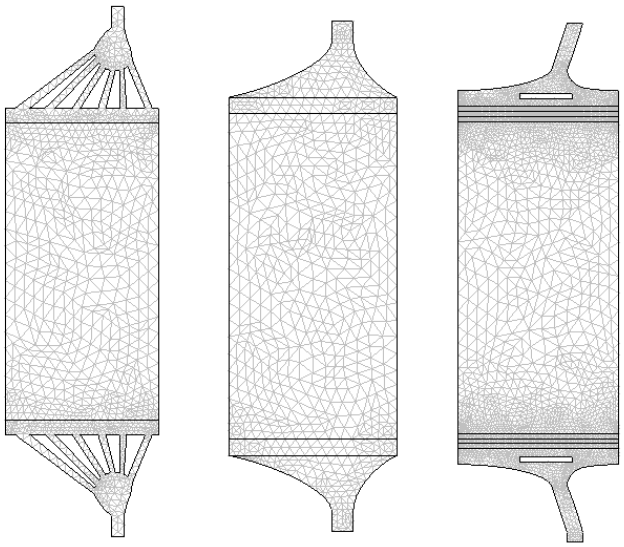

FIGURE 3. Geometries and meshes used in the simulations of designs A, B1, B2 and C from left to right.

2.6. *Results from theoretical study*

The calculated flow distributions were compared by sampling the streamwise velocity, V_{CL}, along lines of constant stream wise position in the active area

of the module. In figure 4 the stream wise velocity, V_{CL}, distribution obtained by solving both thin film theory equations (TFT) and the averaged Navier-Stokes equations for cases B1 and B2 are plotted. The shape of the velocity distribution looks qualitatively the same using both sets of equations but the distribution obtained with the TFT equations is more uniform. When comparing the different designs the results obtained with the averaged Navier-Stokes equations was used since according to the results it represents the worst case scenario.

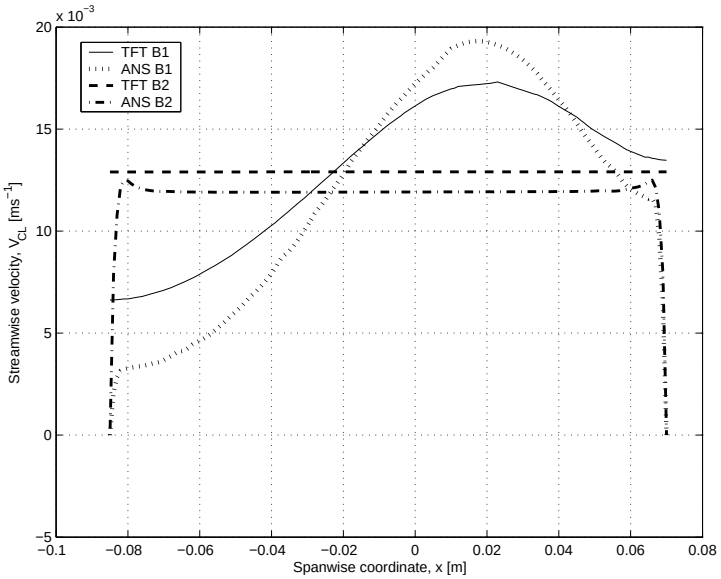

FIGURE 4. Comparison between the TFT equations and the averaged Navier-Stokes equations for cases B1 and B2. The streamwise velocity, V_{CL} calculated using both sets of equations are plotted as a function of x along the dashed line I in figure 2.

In figure 5 the streamwise velocity, V_{CL}, is plotted as a function of spanwise coordinate, x, along the dashed line I in figure 2. The best distribution was obtained with design B2. The distributions obtained with A and C are non-uniform but compared to design B1 a better utilisation of the active area close to the edges of the compartment. The distributions obtained with designs A and C could certainly be made more uniform by optimising their design parameters.

Two cm downstream in the active area, which corresponds to about 6 % of the module length; the streamwise velocity is much more uniform, as can be seen in figure 6.

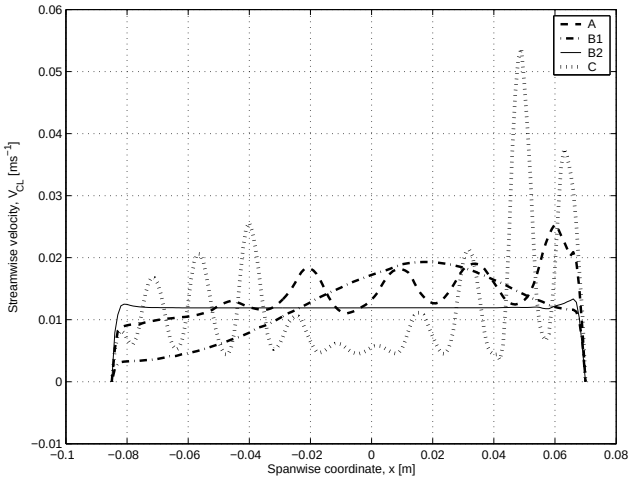

FIGURE 5. Streamwise velocity against spanwise coordinate along the line indicated by I in figure 2.

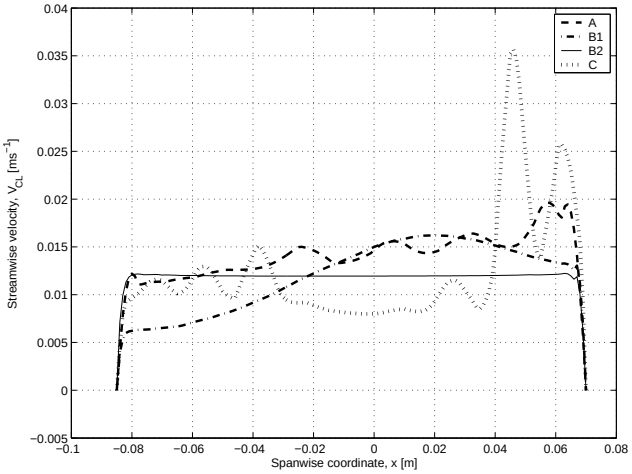

FIGURE 6. Streamwise velocity against spanwise coordinate along the dashed line indicated by II in figure 2.

From these results it was concluded that the flow distribution provided by all the proposed designs was rather uniform. This is due to the relatively narrow flow channels, resulting in a high resistance to the flow from the wall friction. A simplified version of design B, shown in figure 7, was proposed. The advantage of this design was that is was easier to construct. Simulations of

the flow distribution of this frame was conducted and satisfactory results were obtained. This design was chosen for the frame prototype.

The simulations presented here were based on the simplifying assumptions of a fully developed Poiseuille flow in the channels. However, the obtained flow distributions enabled a qualitative comparison of the suitability of the different frame designs.

A drawing of the final design is shown in figure 7 and a photo of the frame with textile in place is shown in figure 8.

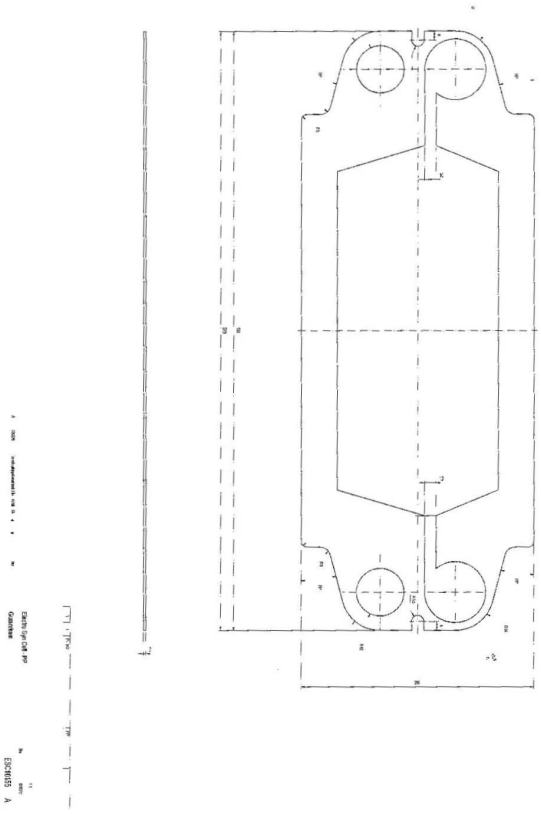

FIGURE 7. Drawing of the prototype frame.

2.7. *Flow visualisation test*

The flow distribution obtained with the manufactured cell was visualised using a plexiglass cover over the ElectroSynCell®. A red tracer color was introduced to the flow just before the inlet to the cell and the distribution of the color gave

an indication of the quality of the flow distribution. In figure 9 a photo from one of these experiments with an empty cell is shown. The introduction of a spacer such as a net or a textile would, ideally, make the flow distribution even more uniform. When the textile was incorporated in the module the increased pressure required to obtain a relevant flow rate caused the transparent plexiglass cover to bend. This made the flow distribution with textile incorporated to appear less uniform.

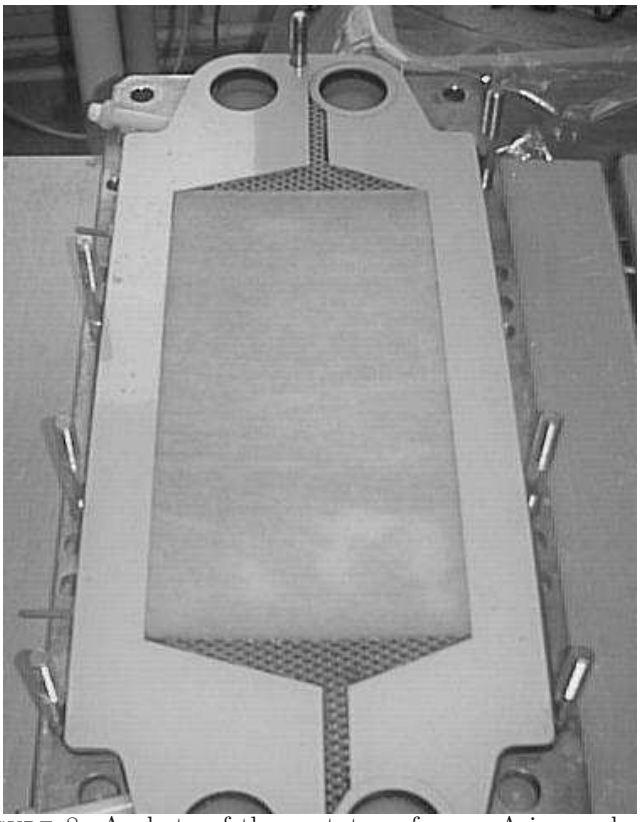

FIGURE 8. A photo of the prototype frame. A ion-exchange textile is placed as spacer over the active area and net-type spacers are incorporated in the inlet and outlet sections.

3. Summary

A electrodialysis module for incorporation of a four mm thick ion-exchange textiles was designed. The design was based on the ElctroSynCell design and new thinner frames were developed. Three different frame designs were proposed and the flow field through them, without ion-exchange textile incorporated, was studied theoretically before a decision on the design of a prototype was

made. An experimental study of the flow distribution was made to ensure that a uniform flow was obtained.

FIGURE 9. Photo from the test of the flow distribution obtained with the developed frames. No ion-exchange textile is incorporated. A spacer net is used in the inlet and outlet section according to figure 8

Acknowledgements

The work was financed by the VINNOVA competence center, FaxénLaboratoriet, with the main industrial partner in this project being Vattenfall AB.

Nomenclature

	Description
Roman letters	
F_x	x component of body force [N/m^3]
F_y	y component of body force [N/m^3]
h	Half height of feed compartment [m]
L	Length of feed compartment [m]
n	Unit outward normal vector [-]
N	Ionic flux [mol/(m^{2}s)]

P	Pressure [Pa]
u	Velocity vector [m/s]
Re	Reynolds number $\frac{\rho u_0 L}{\mu}$ [-]
t	Time [s]
u	Velocity in x-direction [m/s]
U_{CL}	Centerline velocity in x-direction [m/s]
v	Velocity in y-direction [m/s]
V_{CL}	Centerline velocity in y-direction [m/s]
w	Velocity in z-direction [m/s]
x	Coordinate [m]
y	Coordinate [m]
z	Coordinate [m]
Greek letters	
κ	Permeability [m^2]
μ	Dynamic viscosity [Pa s]
ν	Kinematic viscosity [m^2/s]
ρ	Density [kg/m^3]
σ	Ratio of thickness to length of feed compartment, $\frac{h}{L}$[-]
Subscript	
Superscript	
*	Value taken at phase-interface
-	Referes to textile-phase
$\sim$	Non dimensional variable
m	Referes to membrane

References

Acheson, D. 1990 *Elementary Fluid Dynamics*. Claredon Press, Oxford.

Belfort, G. 1972 An experimental study of electrodialysis hydrodynamics. *Desalination* **10** (221-262).

Bengoa, C., Montillet, A., Legentilhomme, P. & Legrand, J. 1997 Flow visualization and modelling of a filter-press type electrochemical reactor. *Journal of Applied Electrochemistry* **27**, 1313–1322.

Bengoa, C., Montillet, A., Legentilhomme, P. & Legrand, J. 2000 Characterisation and modelling of the hydrodynamic behaviour in the filter-press type FM01-LC electrochemical cell by direct flow visualization and residence time distribution. *Ind. Eng. Chem. Res.* **39**, 2199–2206.

Cao, Z., Wiley, D. & Fane, A. 2001 Cfd simulations of net-type turbulence promoters in a narrow channel. *Journal of Membrane Science* **185**, 157–176.

Carlsson, L., Holmberg, H., Johansson, B. & Nilsson, A. 1982 *Techniques of Electroorganic Synthesis Part III, N.L. Weinberg & B.V. Tilak*, chap. III. John Wiley & sons.

Carlsson, L., Sandegren, B., Simonsson, D. & Rihovsky, M. 1983 Design and performance of a modular, mulit-purpose electrochemical reactor. *J.Electrochem.Soc.* p. 342.

Darcovich, K., Dal-Cin, M., Ball´evre, S. & Wavelet, J.-P. 1997 Cfd-assisted thin channel membrane characterization module design. *Journal of membrane Science* **124**, 181–193.

Karode, S. K. & Kumar, A. 2001 Flow visualization through spacer filled channels by computational fluid dynamics i. pressure drop and shear rate calculations for flat sheet geometry. *Journal of Membrane Science* **193** (69-84).

Kho, T. & Muller-Steinhagen, H. 1999 An experimental and numerical investigation of heat transfer fouling and fluid flow in flat plate heat exchangers. *Trans IChemE* **Vol 77** (A2), 124–130.

Pellegrin, E., Michelitsch, E., Darcovich, K., Lin, S. & Tam, C. 1995 Turbulent transport in membrane modules by cfd simulation in two dimensions. *Journal of Membrane Science* **100**, 139–153.

Schoebesberger, H., Einzmann, M., Schmidtbauer, J., Gayrine, P. & Martinetti, R. 2004 Iontex-viscose fibers with ion exchange properties. *Chemical Fibes International* **54** (2), 101–111.

Paper 2

2

Nitrate Removal by Continuous Electropermutation Using Ion-Exchange Textile Part I: Modeling

By Carl-Ola Danielsson[1], Anders Dahlkild[1], Anna Velin[2] & Mårten Behm[3]

A steady state model of the feed compartment and adjacent membranes in a electropermutation cell, used for nitrate removal, with ion-exchange textiles incorporated as a conducting spacer is developed. In the model the ion-exchange textile is treated as a porous media and volume averaging is applied to obtain a macro-homogeneous two-phase model. The ion-exchange between the two phases is modeled assuming that the rate determining step is the mass transfer resistance on the liquid side of the phase interface. Analysis of the model equations revels appropriate simplifications. The influence of the governing dimensionless numbers is investigated through simulations based on the model.

1. Introduction

Excessive use of fertilisers in agricultural activities has caused the nitrate concentration in ground and surface water to increase. According to the *Guidelines for drinking water quality* set up by WHO (2004) the nitrate level in drinking water should not exceed 50 ppm. In the EU the regulated maximum level of nitrate in drinking water is 50 ppm but the recommendations is for less than 25 ppm.

Different techniques are available for nitrate removal from water; biological, chemical and physiochemical such as Donnan dialysis, electrodialysis, electrodeionisation, reverse osmosis and ion-exchange (Salem *et al.* 1995).

Ion-exchange represents the most widespread method for nitrate removal. The problem with ion-exchange is that it is not a continuous process. The ion-exchange material eventually becomes exhausted; the process then has to be stopped and the ion-exchanger material regenerated. Electrodialysis on the other hand is a continuous separation technique; however treating solutions with poor conductivity with electrodialysis is not very efficient.

[1]Department of Mechanics, KTH, SE-100 44 Stockholm, Sweden.
[2]Vattenfall Utveckling AB, SE-100 00 Stockholm, Sweden.
[3]Department of Chemical Engineering and Technology, KTH, SE-100 44 Stockholm, Sweden.

Hybrid ion-exchange/electrodialysis processes, capable of treating solutions of low conductivity in a continuous way, has been investigated since the mid 1950s for various applications (Walters *et al.* 1955). The use of ion-exchange textiles instead of ordinary ion exchange resins has been proposed (Dejean 1997; Dejean *et al.* 1997, 1998; Laktionov *et al.* 1999). The main advantages of using ion-exchange textiles instead of resins are higher permeability, faster ion-exchange kinetics, better contact with the membranes and easier handling. The diameter of the fibers in the textile is about one order of magnitude less than the diameter of ordinary ion-exchange resin beads. This gives a higher ion-exchange kinetics and a better contact with the membranes. The hydrophilicity of the fibers and high porosity of the textile explains the higher permeability compared to a bed of ion-exchange resins. The inherent uniform structure of the textile leads to less risk for the formation of preferential flow paths resulting in a better utilisation of the ion-exchange material. Ezzahar *et al.* (1996) used ion-exchange textiles in an electromembrane cell in a process they called continuous electropermutation.

The main idea behind continuous electropermutation is to replace either the anions or the cations with other anions/cations respectively. A schematic showing the principles of continuous electropermutation for nitrate removal is shown in figure 1. The selective replacement of either anions or cations has the advantage that the conductivity of the water does not decrease dramatically from the inlet to the outlet as can be the case in electrodialysis. When removing nitrates to produce drinking water it can be an advantage that the minerals in the water are preserved as this influences the quality of the product.

A theoretical model would give fundamental understanding of the mechanisms of the process and their interactions. Simulations could be used to design the equipment as well as optimising operation conditions. In this paper a steady state model for the removal of nitrate from ground water using continuous electropermutation with anion-exchange textile incorporated in the feed compartment is presented.

The vast majority of the publications on ion-exchange/electromembrane process have been experimental works on production of ultra-pure water. The theory of these hybrid processes was first investigated by Glueckauf (1959) in the late 1950s. He proposed a theoretical model where the process was divided into two stages. First the mass transfer to the surface of the ion-exchange resins and then the transfer of ions in a chain of ion-exchange resin beads. Rubinstein (1977) published a theoretical work on a process where ion-exchange fibers was combined with electrodialysis. The objective of his study was to obtain voltage against current curves and thus concentration changes in the bulk were neglected. Macro-homogeneous equations was formed by volume averaging over each phase.

There are some theoretical works on the use of electrodeionisation with ion-exchange resins as conductive spacers for production of ultrapure water (Johann & Eigenberger 1993; Thate 1998; Verbeek *et al.* 1998). A model for continuous

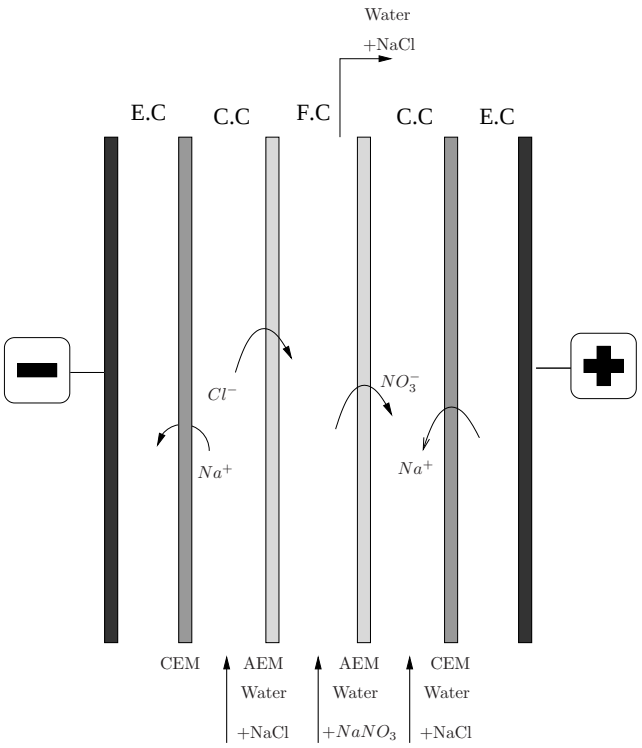

FIGURE 1. The principles behind nitrate removal by continuous electropermutation. The water to be treated through the feed compartment which is separated from the concentrate compartments by anion permeable membranes on each side. The solution in the concentrate compartment has a high concentration of anion A. Under the influence of an applied electric field the anions in the water in the feed compartment are exchanged for anions from the concentrate compartment

electropermutation with ion-exchange textile was presented by Kourda (2000) in her thesis. Macro-homogeneous model equations were presented but not analysed and no results from 2-D simulations were presented. In the model presented here all equations are derived from the microscopic scale and the difficulties introduced by the heterogeneous structure of the fiber net-work is discussed. The obtained macro-homogeneous equations are analysed and appropriate simplifications are motivated.

In a following paper an experimental study of the continuous electropermutation process using ion-exchange textile as conducting spacer is presented. The model predictions and the experimental results will be compared as to

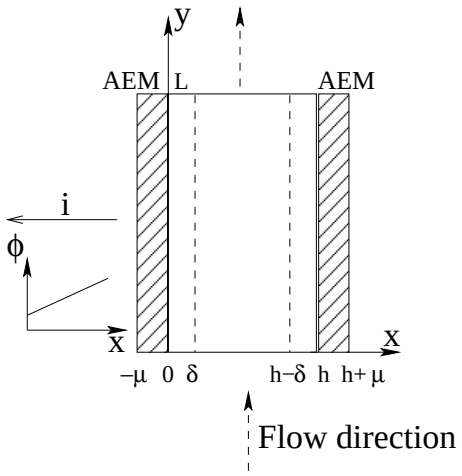

FIGURE 2. The domain included in the model, the feed compartment filled with anion-exchange textile and adjacent ion-exchange membranes. The direction of the current and the flow are indicated in the figure.

validate the model. A future improvement of the model will include the effects of water splitting and the heterogeneous structure of the ion-exchange textile.

2. The Problem Formulation

A steady state model of the feed compartment(F.C.) with adjacent membranes in an electropermutation cell will be formulated. The F.C. is filled with an anion-exchange textile material. A schematic of the domain to be modeled is shown in figure 2 together with the coordinate system used in the model.

The raw water in the model contains low levels of sodium-nitrate and sodium-chloride, thus the ionic species that will be included in the model are NO_3^-, Cl^-, Na^+.

The domain included in the model is divided into three different subdomains i.e. the membrane on the cathodic side, the feed compartment and the membrane on the anodic side. The liquid saturated textile network is assumed to consist of three phases. The fluid which is flowing through the compartment is a liquid mobile phase denoted as the α-phase. The ion-exchange fibers is a solid stationary phase which will be treated as an isotropic porous material, designated as the β-phase. Finally it is assumed that each fibre is surrounded by a stagnant fluid layer of thickness δ, this is the γ-phase.

A schematic picture of the porous media is presented in figure 3. The governing equations are the conservation of mass of each specie and of electric charge in each phase at a microscopic level, together with electroneutrality in

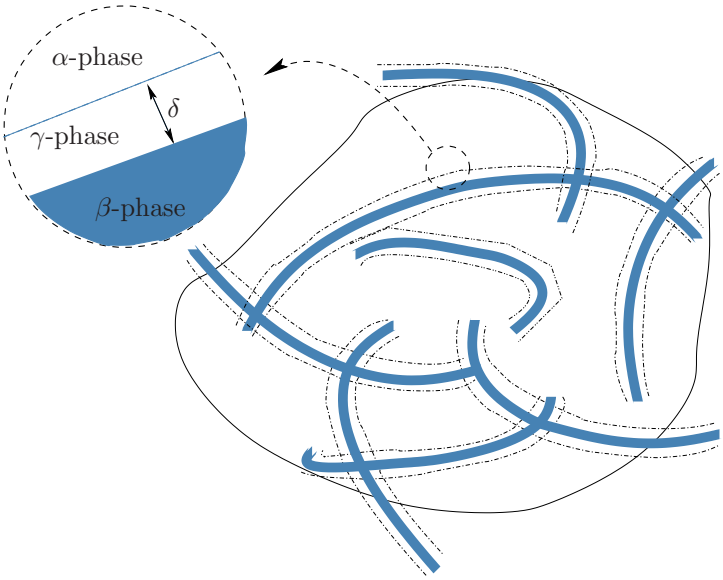

FIGURE 3. Schematic of the textile porous material.

each phase. The governing equations on the macroscopic level are obtained by volume averaging the equations on the microscopic scale.

Two hypotheses were formulated by Rubinstein (1977) which will also be used here.

H1 The overlap of the stagnant layers can be neglected , i.e. each individual fiber can be treated separately, interacting with other fibers only through the α phase.

H2 The ionic transfer along the fibres in the stagnant layer can be neglected; compared to the ionic transfer in that direction in the other two phases.

These two hypotheses require that the volume fraction of fibres in the feed compartment is sufficiently low. The second hypothesis allows us to reduce the model from three phases to two phases. A simplified Nernst diffusion layer model will replace the γ-phase in the model equations and the transport over the γ phase will enter our model as the coupling between the liquid and the textile phases. The volume fraction of the γ phase is small and will be neglected.

2.1. *Governing equations in the membranes*

The membranes are treated as solid electrolytes with a homogeneous distribution of fixed charges. Furthermore it is assumed that the membranes are perfectly ideal so that no co-ions are allowed to pass through the membranes.

2.1.1. *Electroneutrality*

Throughout the model it is assumed that electroneutrality prevails, in the membrane this gives,

$$\sum_i z_i c_i^m + z_{mem}^m c_{mem}^m = 0 \quad \text{for } i = 1, 2 \tag{1}$$

with i equal to 1 and 2 referring to NO_3^- and Cl^- respectively. z_{mem}^m and c_{mem}^m are the valence and concentration of the fixed charges in the membranes. The superscript m refers to values in the membranes.

2.1.2. *Conservation of mass*

Mass conservation at steady state in the membranes is described by,

$$\nabla \cdot \mathbf{N}_i^m = 0 \quad i = 1, 2. \tag{2}$$

The fluxes in the membrane are assumed to be described by the Nernst-Planck equation

$$\mathbf{N}_i^m = \underbrace{-D_i^m \nabla c_i^m}_{\text{Diffusion}} \underbrace{- z_i u_i^m c_i^m \nabla \phi^m}_{\text{Migration}}. \tag{3}$$

The convective flow through the membranes could be modeled by Schlögel's equation (Schlöel & Schöedel 1955). In the present model it is however assumed that the convection in the membranes can be neglected. The current density in the membranes can be expressed using Faraday's law,

$$\mathbf{i}^m = F \sum_{i=1}^{2} z_i \mathbf{N}_i^m. \tag{4}$$

The concervation of electric charge,

$$\nabla \cdot \ \mathbf{i}^m = 0, \tag{5}$$

is nothing else than a linear combination of the equations for conservations of mass. For the three unknowns c_1^m,c_2^m and ϕ^m in the membranes two differential equations and the electroneutrality condition need to be solved.

2.2. *Governing equations in the feed compartment*

2.2.1. *Electroneutrality*

Electroneutrality in the feed compartment gives,

$$\sum z_i c_i = 0 \qquad \text{in the } \alpha \text{ phase for } i = 1 - 3 \tag{6a}$$

$$\sum z_i \bar{c}_i + z_\omega \omega = 0 \qquad \text{in the } \beta \text{ phase for } i = 1, 2 \tag{6b}$$

here i is a number between 1 and 3 referring to NO_3^-, Cl^- and Na^+ respectively. z_i is the valence of the i-th ionic specie, z_ω is the valence of the fixed charges in the ion-exchange fibers and ω is the concentration of functional groups in the ion-exchange fibers. The concentrations c_i and $\bar{c}_i$ are the intrinsic averages of the concentration in each phase.

2.2.2. *Conservation of mass*

Conservation of specie i in the α-phase on the microscopic level at steady state is given by,

$$\nabla \cdot \mathbf{N}_i = 0 \quad \text{for } i = 1 - 3. \tag{7}$$

The ion-exchange textile is treated as an ideally selective ion-exchanger, thus the mass balance equations in the textile-phase are given by

$$\nabla \cdot \bar{\mathbf{N}}_i = 0 \quad \text{for } i = 1, 2 \tag{8}$$

The macro-homogeneous version of the mass conservation equations are obtained by volume averaging the equations at the micro scale. Applying the volume averaging theorem Whitaker (1999) allows the superficial averages of the mass conservation equations to be expressed as,

$$< \nabla \cdot \mathbf{N}_i >= \nabla \cdot < \mathbf{N}_i > + \frac{1}{V} \int_{A_{\alpha,\gamma}} \mathbf{N}_i \cdot \mathbf{n}_{\alpha,\gamma} \, \mathrm{d}A \quad \text{for } i = 1 - 3 \tag{9}$$

Where the integral terms in equations 9 describes the flux over the phase interfaces.

$$\frac{1}{V} \int_{A_{\alpha,\gamma}} \mathbf{N}_i \cdot \mathbf{n}_{\alpha,\gamma} \, \mathrm{d}A = S_i \quad \text{for } i = 1 - 3 \tag{10a}$$

$$\frac{1}{V} \int_{A_{\beta,\gamma}} \bar{\mathbf{N}}_i \cdot \mathbf{n}_{\beta,\gamma} \, \mathrm{d}A = \bar{S}_i \quad \text{for } i = 1 - 3 \tag{10b}$$

A consequence of the second hypothesis is that,

$$S_i = -\bar{S}_i \quad \text{for } i = 1 - 3 \tag{11}$$

where $S_3 = 0$ due to the ideal selectivity of the β-phase.

The interfacial fluxes enters as sink/source terms in the macro-homogeneous equations. Thus conservation of mass at the macroscopic level gives,

$$< \nabla \cdot \mathbf{N}_i >= \nabla \cdot < \mathbf{N}_i > - \bar{S}_i = 0 \quad \text{for } i = 1 - 3 \tag{12}$$

$$< \nabla \cdot \bar{\mathbf{N}}_i >= \nabla \cdot < \bar{\mathbf{N}}_i > + \bar{S}_i = 0 \quad \text{for } i = 1, 2 \tag{13}$$

Conservation of electric charge can be formulated in the same way as for the membrane. The volume average of the conservation of electric charge gives

$$\nabla \cdot < \mathbf{i} >= -\frac{1}{V} \int_{A_{\alpha,\gamma}} \mathbf{i} \cdot \mathbf{n}_{\alpha,\gamma} \, \mathrm{d}A = -F \sum z_i S_i \tag{14a}$$

$$\nabla \cdot < \bar{\mathbf{i}} >= -\frac{1}{V} \int_{A_{\beta,\gamma}} \bar{\mathbf{i}} \cdot \mathbf{n}_{\beta,\gamma} \, \mathrm{d}A = F \sum z_i \bar{S}_i \tag{14b}$$

Summing these equations gives one equation for the total current density

$$\nabla \cdot < \mathbf{i} > + \nabla \cdot < \bar{\mathbf{i}} >= 0. \tag{15}$$

The Nernst-Planck equation is used as the transport equation that describes the ionic fluxes at the microscopic scale. Expressing the superficial volume average of these fluxes in terms of the intrinsic volume averages of

the concentrations and potentials turns out to be a complex problem. In this first attempt to model the feed compartment the volume averaged fluxes are assumed to be described by,

$$< \mathbf{N}_i > = \underbrace{\mathbf{j}c_i}_{\text{Convection}} \underbrace{-\mathcal{D}^{'}\nabla c_i}_{\text{Hydrodynamic Dispersion}} \underbrace{-z_i\frac{F}{RT}D_{i,e}c_i\nabla\phi}_{\text{Effective Migration}} \tag{16a}$$

$$< \bar{\mathbf{N}}_i >= \underbrace{-\bar{D}_{i,e}\nabla\bar{c}_i}_{\text{Effective Diffusion}} \underbrace{-z_i\frac{F}{RT}\bar{D}_{i,e}\bar{c}_i\nabla\bar{\phi}}_{\text{Effective Migration}} \tag{16b}$$

The superficial average of the fluid velocity, $\mathbf{j}$, is calculated as the volumetrical flow rate divided by the cross section area of the empty channel. c_i and $\bar{c}_i$ are the intrinsic averages of the concentrations of specie i in the α and β-phases respectively. The reason for using the intrinsic averages of the concentrations is that it is this concentration that can be measured. $D_{i,e}$ and $\bar{D}_{i,e}$ are the effective diffusion coefficients of specie i in the α and β phase respectively. $\mathcal{D}^{'}$ is the hydrodynamic dispersion tensor.

The structure of the porous media will influence the ionic transport through it. In this model it is assumed that the two macro-homogeneous phases are arranged in parallel with each other (Kourda 2000; Dejean 1997).

The effective diffusion coefficients are modeled by (Bird *et al.* 2002)

$$D_{i,e} = \frac{\epsilon_\alpha}{\tau_\alpha}D_i \tag{17a}$$

$$\bar{D}_{i,e} = \frac{\epsilon_\beta}{\tau_\beta}\bar{D}_i \tag{17b}$$

where τ_α, τ_β are the tortuosities and ϵ_α and ϵ_β are the volume fractions of the porous material in respective phase. The tortuosity is generally considered to be dependent on the porosity and thus the effective diffusion coefficient is often modeled as (Newman 1991)

$$D_{i,e} = \epsilon_\alpha^{1+b}D_i. \tag{18a}$$

For simplicity it is assumed that the same models can be used also in the ion-exchange phase.

$$\bar{D}_{i,e} = \epsilon_\beta^{1+b}\bar{D}_i \tag{18b}$$

where b is a constant normally set equal to 0.5.

In the migration term the Nernst-Einstein correlation between the mobility and the diffusivity,

$$u_i = \frac{F}{RT}D_i, \tag{19}$$

is used. Here the ionic mobility, u_i is defined according to Helfferich (1995).

In a uniaxial flow along the y-axis through an isotropic porous material the dispersion tensor is given by,

$$\mathcal{D} = \begin{pmatrix} \mathcal{D}_T & 0 & 0 \\ 0 & \mathcal{D}_L & 0 \\ 0 & 0 & \mathcal{D}_T \end{pmatrix} \tag{20}$$

where $\mathcal{D}_L$ is known as the longitudinal coefficient of dispersion and $\mathcal{D}_T$ as the transverse coefficient of dispersion. The values of $\mathcal{D}_L$ and $\mathcal{D}_T$ are determined experimentally and in the literature a number of correlations can be found. Usually it is the coefficient of hydrodynamic dispersion,

$$\mathcal{D}_{\mathcal{L}}{}' = (\mathcal{D}_{\mathcal{L}} + D_{i,e}),$$

that is given. Here the following correlations will be used (Bear 1988; Dullien 1992),

$$\mathcal{D}_L' = 2.7\, D_0\, Pe_{df} \quad \text{for } 300 < Pe_{df} < 10^4 \tag{21a}$$

where Pe_{df} is the Peclet number based on the diameter of the fibers in the β phase and D_0 is a reference molecular diffusivity.

$$Pe_{df} = \frac{j_0 d_f}{D_0}$$

For the transverse coefficient less experiments are available. However one could expect a similar relationship to Pe_{df} as for the longitudinal coefficient of dispersion (Bear 1988). For the ratio $\frac{\mathcal{D}_L}{\mathcal{D}_T}$ values from 3 up to 24 (Greenkorn 1983; Dullien 1992) are found in the literature. Using a value of 10 for this ratio gives,

$$\mathcal{D}_T' = 0.27\, D_0\, Pe_{df} \quad \text{for } 300 < Pe_{df} < 10^4 \tag{21b}$$

2.2.3. *A Model for the ion-exchange rate*

A study of the ion-exchange kinetics on ion-exchange fibers made by Petruzzelli *et al.* (1995) suggested that the rate determining step for the ion-exchange is associated with the mass transfer on the liquid side.

The sink/source terms in the volume averaged mass balance equations are calculated from

$$\bar{S}_i = < N_i >^* \mathfrak{S}_a. \tag{22}$$

where $< N_i >^*$ is the average flux of specie i over the phase interface. The specific surface area of the fibers, $\mathfrak{S}_a$, is taken to be

$$\mathfrak{S}_a = \frac{4}{d_f}\epsilon_\beta \tag{23}$$

where d_f is the fibre diameter.

The average flux over the phase interface is calculated by treating the γ-phase as a Nernst diffusion layer of thickness δ. The fluxes over the Nernst layer is expressed in terms of concentration differences over the layer as,

$$< N_i >^* = \frac{D_i}{\delta}[(c_i^* - c_i) - z_i \frac{c_i^*}{c_3^*}(c_3^* - c_3)] \quad \text{for } i = 1 - 3 \tag{24}$$

where the star indicates the average value taken at the phase interface. In the expression above the ideal selectivity of the textile is used to express the

potential gradient in the terms of the gradient in concentration of the co-ion $i = 3$. Ion-exchange equilibrium prevails at the interface; thus

$$c_2^* = \alpha_2^{\beta 1} \frac{\bar{c}_2}{\bar{c}_1} c_1^* \tag{25a}$$

$$\phi^* = \bar{\phi} + \frac{RT}{F} \ln \frac{c_1^*}{\bar{c}_1}. \tag{25b}$$

where $\alpha_2^{\beta 1}$ is the separation coefficient. For a non-selective anion-exchanger, $\alpha_2^{\beta 1} = 1$.

The thickness of the Nernst layer, δ, is assumed to be controlled by the hydrodynamics and hence the same value is used for all ionic species. The ion-exchange rate is thus expressed as

$$\bar{S}_i = \frac{4\epsilon_\beta D_i}{d_f \delta} \left(\Delta c_i - z_i \frac{c_i^*}{c_3^*} \Delta c_3 \right) \quad \text{for } i = 1 - 3 \tag{26}$$

where $\Delta c_i = c_i^* - c_i$.

An estimate of the thickness of the stagnant layer is obtained from the following correlation,

$$Sh = \frac{1.09}{\epsilon_\alpha} (Re_d Sc)^{\frac{1}{3}} \tag{27}$$

where $Sh = \frac{kd}{D} = \frac{d}{\delta}$, $Sc = \frac{\nu}{D}$, $Re_d = \frac{jd}{\nu}$. This correlation was obtained from experiments with a packed bed of spheres with a diameter d (Wilson & Geankoplis 1966). To use this correlation for our fibrous bed, a diameter of a fictitious sphere having the same specific area as our fibers is used.

2.2.4. *The boundary layers*

Close to the membranes the convective transport goes down to zero at the same time as the mechanical dispersion vanishes. Thus there will be a boundary layer in which the molecular diffusion becomes important. Instead of resolving the boundary layer numerically a Nernst diffusion layer model is used. The transport equations in the boundary layer are expressed as,

$$N_i = -D_{i,e} \nabla c_i - z_i \frac{F}{RT} D_{i,e} c_i \nabla \phi \tag{28a}$$

$$\bar{N}_i = -\bar{D}_{i,e} \nabla \bar{c}_i - z_i \frac{F}{RT} \bar{D}_{i,e} \bar{c}_i \nabla \phi \tag{28b}$$

The gradients in the Nernst-layer are assumed to be constant.

An estimate for the thickness of the concentration boundary layer close to the walls in a porous bed was presented by Koch Koch (1996),

$$\delta_c = \xi \left(\frac{D}{\mathcal{D}_\infty} \right)^{1/3} \sim \xi \left(0.27 Pe_{d_f} \right)^{-1/3} \tag{29}$$

where ξ is a characteristic length scale of the porous bed. This characteristic length is often taken as the square root of the permeability, κ, of the porous media.

The concentrations and the potential on each side of the diffusion layer are obtained from the solution of the equations in the membrane and in the feed compartment.

2.3. *Boundary conditions*

The composition of the water to be treated has to be specified which gives the boundary conditions at the inlet boundary,

$$c_i|_{0\le x\le h, y=0} = c_{i0} \quad \text{for } i = 1-3. \tag{30}$$

The change of the composition in the flow direction is taken to be negligible at the outlet boundary,

$$\frac{\partial c_i}{\partial y}|_{0\le x\le h, y=L} = 0 \quad \text{for } i = 1-3. \tag{31}$$

The composition of the solution on the concentrate side of the membrane is assumed to be known and constant along the length of the channel. This can be justified by having a concentration many times higher than in the feed compartment. It is assumed that ion-exchange equilibrium prevails at interface between membrane and the concentrate compartment. Furthermore the potential in the membranes at the interface with the concentrate compartments are prescribed. This gives the necessary boundary conditions at $x = -\mu$ and $x = h + \mu$,

$$c_1^m|_{x=-\mu,h+\mu,0\le y\le L} = \frac{\alpha_2^{m1} c_{1c} c_{mem}^m}{c_{2cc} + \alpha_2^{m1} c_{1cc}} \tag{32a}$$

$$c_2^m|_{x=-\mu,h+\mu,0\le y\le L} = \frac{c_{2cc} c_{mem}^m}{c_{2cc} + \alpha_2^{m1} c_{1cc}} \tag{32b}$$

$$\phi^m|_{x=-\mu,0\le y\le L} = 0 \tag{32c}$$

$$\phi^m|_{x=h+\mu,0\le y\le L} = \phi_0 \tag{32d}$$

At the internal boundaries between the membranes and feed compartment all ionic fluxes and electrochemical potentials are continuous.

$$c_1^m|_{x=0,h,0\le y\le L} = \frac{\alpha_2^{m1} c_1 c_{mem}^m}{c_2 + \alpha_2^{m1} c_1} \tag{33a}$$

$$c_2^m|_{x=-0,h,0\le y\le L} = \frac{c_2 c_{mem}^m}{c_2 + \alpha_2^{m1} c_1} \tag{33b}$$

$$\phi^m|_{x=0,h,0\le y\le L} = \phi + \frac{RT}{F} \ln \frac{c_1^m}{c_1} \tag{33c}$$

where it has been assumed that the activity coefficient in the membrane and the α-phase takes the same value at the interface.

3. Analysis

To analyze the equation and motivate possible simplifications the model equations are made dimensionless.

3.1. *Membrane equations*

The equations in the membranes are made dimensionless by introducing the following dimensionless variables,

$$\begin{aligned} \tilde{x} = \frac{x}{\mu},\ \tilde{y} = \frac{y}{L},\ \sigma_m = \frac{\mu}{L} \\ X_i^m = \frac{c_i^m}{c_0^m},\ \Phi^m = \frac{\phi^m}{\phi_0} \end{aligned} \tag{34}$$

and a dimensionless diffusion coefficient

$$\tilde{D}_i^m = \frac{D_i^m}{D_0^m} \tag{35}$$

3.1.1. *Electroneutrality*

The concentrations in the membrane are scaled with the concentration of the fixed charges. This gives that the non-dimensional electroneutrality condition in the membrane can be expressed as,

$$X_1^m + X_2^m = 1 \tag{36}$$

3.1.2. *Conservation of mass*

$$\tilde{D}_i^m \left(\frac{\partial^2 X_i^m}{\partial \tilde{x}^2} + \sigma_m^2 \frac{\partial^2 X_i^m}{\partial \tilde{y}^2} \right) + z_i \mathcal{V}^m \tilde{D}_i^m \left[\frac{\partial}{\partial x} \left(X_i \frac{\partial \Phi^m}{\partial \tilde{x}} \right) + \sigma_m^2 \frac{\partial}{\partial y} (X_i \frac{\partial \Phi^m}{\partial \tilde{y}} \right) \Bigg] = 0 \tag{37}$$

where $\mathcal{V}^m = \frac{F\phi_0}{RT}$.

The membranes are very thin, which makes σ_m small. Neglecting terms multiplied by σ_m^2 is essentially the same as treating the membrane as one-dimensional and only consider transport in the x direction. The steady state version of the equation is then given by

$$\frac{\partial^2 X_i^m}{\partial \tilde{x}^2} + z_i \mathcal{V}^m X_i^m \frac{\partial^2 \Phi^m}{\partial \tilde{x}^2} = 0 \tag{38}$$

Writing the fluxes in the membrane in terms of the dimensionless variables yields

$$N_{i,x}^m = -\frac{D_0^m c_0^m}{\mu} \tilde{D}_i^m \left(\frac{\partial X_i}{\partial \tilde{x}} + z_i \mathcal{V}^m X_i \frac{\partial \Phi^m}{\partial \tilde{x}} \right) \tag{39}$$

Order of magnitude estimates of the membrane parameters gives (Elattar *et al.* 1998)

$$D_0^m = O(10^{-11})[\mathrm{m^2\,s}],\ \mu = \mathrm{O}(10^{-4})[\mathrm{m}],\ \mathrm{c_0^m} = \mathrm{O}(10^3)[\mathrm{mol\,m^{-3}}]. \tag{40}$$

The maximum nitrate flux through the membrane which can be obtained without applying an electric field is estimated as

$$N_{1,x}^m = \frac{D_0^m c_0^m}{\mu} = O(10^{-4})[\mathrm{mol} s^{-1} m^2]. \tag{41}$$

This is the flux obtained when one side of the membrane is full of nitrate and the other side is completely free from nitrate. This is almost the situation in the beginning of the cell where the molar fraction of nitrate is high in the raw water entering the feed compartment and low in the concentrate solution. Assuming that this flux would be obtained over the total membrane surface one get an estimate of the total amount of nitrate that can be removed via Donnan dialysis; this should be compared to the total amount of nitrate that enters the feed compartment.

$$\Delta = \frac{2LD^m c_0^m}{\mu j_0 h c_0} = \frac{2D^m c_0^m}{\mu \sigma j_0 c_0} \tag{42}$$

where $\sigma = \frac{h}{L}$. The larger this number is the more important the nitrate removal via Donnan dialysis becomes.

According to the model equations it should be possible to remove nitrate from the feed compartment by diffusion even if the absolute concentration of nitrate outside the membrane is higher than inside the dilute compartment. This is due to the high concentration difference of chloride over the membrane which drives a flux of nitrate in the opposite direction in order for electroneutrality to prevail.

3.2. *Feed compartment equations*

The following dimensionless variables are introduced,

$$\begin{aligned} &\tilde{x} = \frac{x}{h},\ \tilde{y} = \frac{y}{L},\ \tilde{\mathbf{j}} = \frac{\mathbf{j}}{j_0},\ X_i = \frac{c_i}{c_0}, \\ &Y_i = \frac{\bar{c}_i \epsilon}{w \rho_\beta},\ \Phi = \frac{\phi}{\phi_0},\ \bar{\Phi} = \frac{\phi}{\phi_0},\ \epsilon = \epsilon_\beta = (1 - epsilon_\alpha) \end{aligned} \tag{43}$$

together with the dimensionless diffusion coefficients

$$\tilde{D}_i = \frac{D_i}{D_0},\ \tilde{\bar{D}}_i = \frac{\bar{D}_i}{D_0}. \tag{44}$$

Values for the diffusion coefficient of the pure liquid, D_i, can be found in the literature. The mobility of ions inside the fibers are lower due to the friction caused by the backbone of the fibers and the electrostatic attractions of the fixed groups (Helfferich 1995). In the analysis of the model equations the following relationship between the diffusion coefficients will be used,

$$\bar{D}_i = 0.15 D_i. \tag{45}$$

The flow through the textile is treated as a plug flow in the y-direction, thus $\tilde{\mathbf{j}} = (0, \tilde{j}_y, 0)$.

3.2.1. *Electroneutrality*

The non-dimensional electroneutrality conditions in the feed compartment are given by

$$X_1 + X_2 = X_3 \tag{46}$$

$$Y_1 + Y_2 = 1 \tag{47}$$

3.2.2. *Conservation of mass*

Using the dimensionless variables and coefficients one can express the macro-homogeneous conservation of mass equations as,

$$\tilde{j}_y \frac{\partial X_i}{\partial \tilde{y}} - 2.7\vartheta \frac{\partial^2 X_i}{\partial \tilde{y}^2} - 0.27\frac{\vartheta}{\sigma^2}\frac{\partial^2 X_i}{\partial \tilde{x}^2} -$$

$$- z_i \frac{\mathcal{V}(1-\epsilon)^{1.5}\tilde{D}_i}{\sigma^2 Pe}\left[\frac{\sigma^2\partial}{\partial\tilde{y}}\left(X_i\frac{\partial\Phi}{\partial\tilde{y}}\right) + \frac{\partial}{\partial\tilde{x}}\left(X_i\frac{\partial\Phi}{\partial\tilde{x}}\right)\right] + \frac{4\,\epsilon\tilde{D}_i}{\vartheta^2 Pe}\frac{\tilde{\bar{\mathcal{S}}}_i}{\tilde{\delta}} = 0 \text{ for } i = 1-3 \tag{48a}$$

$$-\frac{0.15\epsilon^{1.5}Z\tilde{D}_i}{\sigma^2 Pe}\left(\frac{\sigma^2\partial^2 Y_i}{\partial\tilde{y}^2} - \frac{\partial^2 Y_i}{\partial\tilde{x}^2}\right) - z_i\frac{0.15\mathcal{V}\epsilon^{1.5}Z\tilde{D}_i}{\sigma^2 Pe}\left[\frac{\sigma^2\partial}{\partial\tilde{y}}\left(Y_i\frac{\partial\bar{\Phi}}{\partial\tilde{y}}\right) + \frac{\partial}{\partial\tilde{x}}\left(Y_i\frac{\partial\bar{\Phi}}{\partial\tilde{x}}\right)\right]$$

$$+ \frac{4\,\epsilon\tilde{D}_i}{\vartheta^2 Pe}\frac{\tilde{\bar{\mathcal{S}}}_i}{\tilde{\delta}} = 0 \text{ for } i = 1,2 \tag{48b}$$

where

$$\tilde{\bar{\mathcal{S}}}_i = \Delta X_i - z_i\frac{X_i^*}{X_{Na^+}^*}\Delta X_{Na^+} \tag{49}$$

Above the following dimensionless parameters were introduced,

$$\sigma = \frac{h}{L},\ \vartheta = \frac{d_f}{L},\ \mathcal{V} = \frac{F\phi_0}{RT},\ Z = \frac{\omega\rho_\beta}{\epsilon c_0},\ Pe = \frac{j_0 L}{D_0},\ \tilde{\delta} = \frac{\delta}{d_f} \tag{50}$$

The long and slender geometry can be used to simplify the equations. Consider the limit when $\sigma^2 \to 0$ at the same time as $\vartheta \to 0$ so that $\frac{\vartheta}{\sigma^2} = \theta =$ constant. Furthermore $Pe \to \infty$ in such a way that $\sigma^2 Pe = \tilde{Pe} =$ constant. The parameter $\mathcal{V}$,ϵ_β and $\tilde{D}_i$ are kept constant as $\sigma^2 \to 0$. In this limit the mass balance equations with $\tilde{j} = 1$ can be written as,

$$\frac{\partial X_i}{\partial\tilde{y}} - 0.27\theta\frac{\partial^2 X_i}{\partial\tilde{x}^2} - z_i\frac{\mathcal{V}(1-\epsilon)^{1.5}}{\tilde{Pe}}\tilde{D}_i\frac{\partial}{\partial\tilde{x}}\left(X_i\frac{\partial\Phi}{\partial\tilde{x}}\right) - \frac{4\,\epsilon}{\sigma^2\theta^2\tilde{Pe}}\tilde{D}_i\frac{\tilde{\bar{\mathcal{S}}}_i}{\tilde{\delta}} = 0 \tag{51a}$$

$$-\frac{0.15\epsilon^{1.5}Z}{\tilde{Pe}}\tilde{D}_i\frac{\partial^2 Y_i}{\partial\tilde{x}^2} - z_i\frac{0.15\mathcal{V}\epsilon^{1.5}Z}{\tilde{Pe}}\tilde{D}_i\frac{\partial}{\partial\tilde{x}}\left(Y_i\frac{\partial\bar{\Phi}}{\partial\tilde{x}}\right) + \frac{4\,\epsilon}{\sigma^2\theta^2\tilde{Pe}}\tilde{D}_i\frac{\tilde{\bar{\mathcal{S}}}_i}{\tilde{\delta}} = 0 \tag{51b}$$

The model equations have now become parabolic instead of elliptic due to the neglected second order derivatives in the streamwise direction. Thus all the boundary conditions at $\tilde{y} = 0$ and $\tilde{y} = 1$ can not be fulfilled, without reinstating the streamwise diffusion close to the inlet and the outlet of the feed compartment. This problem is however not considered in this paper. The parabolic nature of the model equations is used to simplify the numerical solution procedure. Instead of solving the full 2-D problem, we march through the feed compartment solving a sequence of 1-D problems at each streamwise

positions. The upstream solution provides the boundary condition at the next dowstream position. By doing this the boundary condition at $\tilde{y} = 1$ is not needed.

For the equations above to be balanced as $\sigma^2 \to 0$ it is necessary that $\overset{\leftrightharpoons}{\mathcal{S}}_i \to 0$. This leads to the condition that the ion-exchanger is in equilibrium with the solution, i.e.

$$Y_2 = \frac{Y_1 X_2}{X_1}. \tag{52}$$

Using this together with the electroneutrality condition (eq. 47) one finds that once X_1 and X_2 are know so are also Y_1 and Y_2. Hence, the number of unknowns can be reduced from seven to four. Eliminating $\overset{\leftrightharpoons}{\mathcal{S}}_i$ from the mass conservations equations above gives,

$$\begin{aligned}\frac{\partial X_i}{\partial \tilde{y}} =& 0.27\theta \frac{\partial^2 X_i}{\partial \tilde{x}^2} + z_i \chi (1-\epsilon)^{1.5} \tilde{D}_i \frac{\partial}{\partial \tilde{x}} \left(X_i \frac{\partial \Phi}{\partial \tilde{x}} \right) + \\ &+ \frac{0.15\epsilon^{1.5} Z}{\tilde{P}e} \tilde{D}_i \frac{\partial^2 Y_i}{\partial \tilde{x}^2} + z_i 0.15 \chi \epsilon^{1.5} Z \tilde{D}_i \frac{\partial}{\partial \tilde{x}} \left(Y_i \frac{\partial \bar{\Phi}}{\partial \tilde{x}} \right) \quad \text{for } i = 1, 2\end{aligned} \tag{53}$$

$$\frac{\partial X_3}{\partial \tilde{y}} = 0.27\theta \frac{\partial^2 X_3}{\partial \tilde{x}^2} + z_3 \chi (1-\epsilon)^{1.5} \tilde{D}_3 \frac{\partial}{\partial \tilde{x}} \left(X_3 \frac{\partial \Phi}{\partial \tilde{x}} \right) \tag{54}$$

where

$$\chi = \frac{\mathcal{V}}{\sigma^2 Pe} = \frac{\mathcal{V}}{\tilde{P}e}. \tag{55}$$

This dimensionless number includes both design parameters and operation conditions that can be used to optimise the process.

3.3. *Dimensionless Boundary Conditions*

The dimensionless boundary conditions are given by

$$X_{0i}^m|_{x=-\mu,\, x=h+\mu} = \frac{c_i^m}{c_0^m} \quad \text{for } i = 1, 2 \tag{56a}$$

$$\bar{\Phi}|_{x=-\mu} = 0 \tag{56b}$$

$$\bar{\Phi}|_{x=h+\mu} = 1 \tag{56c}$$

The nitrate concentration of the raw water is used to scale the concentrations in the α-phase.

$$X_i|_{y=0} = \frac{c_{0i}}{c_{01}} \quad \text{for } i = 1 - 3 \tag{57}$$

The dimensionless boundary condition at the outlet boundary is given by,

$$\frac{\partial X_i}{\partial \tilde{y}}|_{y=L} = 0 \quad \text{for } i = 1 - 3. \tag{58}$$

this is however not used since the second order derivatives in the streamwise direction have been neglected.

4. Result and Discussion

From the analysis of the model equations it was found that the continuous electropermutation process, using non-selective membranes and a non-selective ion-exchange textile as conducting spacer, can essentially be described by three dimensionless numbers: χ,Δ and Z. Both χ and Δ contain the design parameter σ, giving the ratio between the height and the length of the active part of the feed compartment. Operation conditions such as potential drop between the outer part of the membranes and flow rate are also included in one or both of these numbers. Z gives the ratio between the intrinsic averages of the concentrations in the raw water to that of the functional groups in the ion-exchanger. This is a design parameter of the ion-exchange material including porosity, capacity and density of the ion-exchange textile.

The model equations were discretised using a conservative finite volume scheme, which is second order accurate in the x-direction and first order accurate in the y-direction. The non-linear system of equations obtained was solved using the *fsolve* routine in Matlab. The number of node points used was gradually increased as to obtain grid independent solutions with 40 points is the x-direction and 80 points in the y-direction. The constants presented in table 3 were used to obtain representative values of the non-dimensional parameters. The potential drop flow rate and ion-exchange capacity were varied within a span of physically reasonable values to give a set of combinations of χ, Δ and Z.

The distribution of nitrate ions in the feed compartment is shown in figure 4 for a simulation with χ=0.1 ,Δ=0.125 and $Z = 620$. The anode is located on the right hand side of the feed compartment. Due to the applied electric field the nitrate concentration shifted towards the membrane on the anodic side of the compartment.

Geometry and Operation Conditions	
h	3 [mm]
L	0.3 [m]
T	298 [K]
$\mathbf{j}_y$	0.01-0.1 [ms^{-1}]
ϕ_0	0-4 [V]
c_{01}	1.6 [mM]
Textile and membrane parameters	
d_f	12 [μm]
μ	200 [μm]
c^m_{mem}	1 [M]
w	0.0016-2.4 [mol/kg]
ρ_β	150 [kg/m^3]
Physical parameters	
D_1	$1.902 \cdot 10^{-9}$ [m^{2}s^{-1}] Newman (1991)
D_2	$2.032 \cdot 10^{-9}$ [m^{2}s^{-1}] Newman (1991)
D_3	$1.334 \cdot 10^{-9}$ [m^{2}s^{-1}] Newman (1991)
D^m_1	$2.8 \cdot 10^{-11}$ [m^{2}s^{-1}]
D^m_2	$3.9 \cdot 10^{-11}$ [m^{2}s^{-1}]
Non Dimensional Parameters	
σ	10^{-2} [-]
X_{01}	1 [-]
X_{02}	0.1 [-]
X_{03}	1.1 [-]
X^m_{01}	0.1 [-]
X^m_{02}	0.9 [-]
z_1, z_2	-1 [-]
z_3	1 [-]
ϵ	0.15 [-]
χ	0-0.2 [-]
Δ	0.063 - 0.63 [-]
Z	1 - 1500 [-]
α^1_2	1 [-]
α^{m1}_2	1 [-]

TABLE 1. Parameter values used in the simulations.

The local current density in the cell may vary from the inlet to the outlet depending on the composition of the solution. Using electrodialysis one expects the local current density to decrease as one moves towards the outlet of the cell, since the conductivity of the solution decreases with increasing streamwise position. With electropermutation this is not the case and as can be seen in figure 5, where the local current density is plotted as a function of

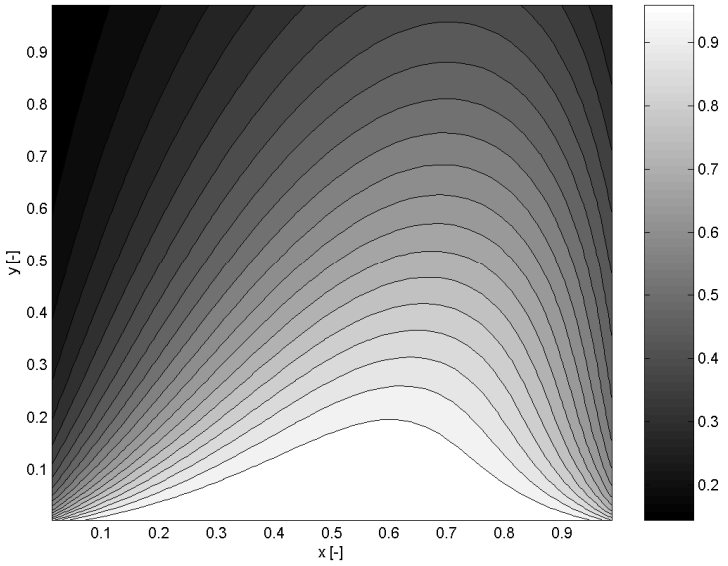

FIGURE 4. The nitrate concentration distribution in the feed compartment at steady state for χ=0.10,Δ = 0.125 and Z=620. The anode is located on the right hand side of the feed compartment.

streamwise position. The local current density increases as one moves from the inlet towards the outlet; due to the gradual replacement of nitrate ions for the slightly more mobile chloride ions. This relatively small change in the conductivity of the feed compartment is one of the advantages of the electropermutation process, since the power consumption can be kept lower compared to electrodialysis.

4.1. *Effect of χ and Δ*

In figure 6 the concentration of nitrate in the product is plotted as function of χ for different values of Δ. It is clear that the nitrate concentration in the product decreases with increasing χ up to a certain point and then levels off. The value of χ where the nitrate concentration levels off represents the optimal value of χ. This can be used to optimise the operation conditions or the design of the equipment. Increasing χ further will only result in a transport of chloride and nitrate ions through the feed compartment.

It is clear that nitrate is removed from the feed compartment even as the value of χ goes to zero. The reason for this is the Donnan dialysis or diffusion dialysis (Mulder 1996). The relative importance of the Donnan dialysis is strongly dependent on the flow rate and composition of the water to be treated as well as the membrane area compared to the thickness of the compartment as is indicated by the dimension less number Δ. The different curves in figure 6

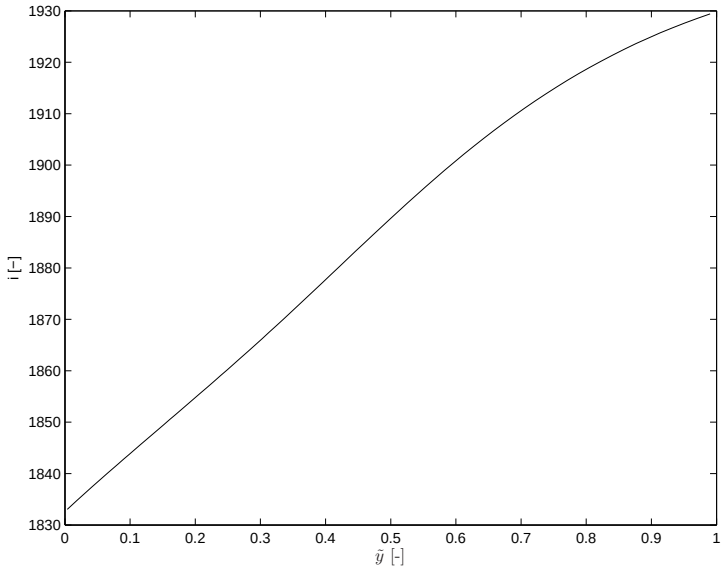

FIGURE 5. The local current density in the cell as a function of streamwise coordinate for χ=0.10, Δ=0.125 and Z=620

represent simulations made for different values of Δ with a constant Z value of 620. For the the higher value of Δ more nitrate is removed by Donnan dialysis as was expected from the analysis of the model equations.

An alternative way to illustrate the result in figure 6 is given in figure 7. Here the contribution to the nitrate removal from different parts of the feed compartments is seen, each line in the plot corresponds to a specific value of χ at a constant Δ value of 0.125 and Z value of 620. For low χ values the nitrate concentration decreases almost linearly from the inlet to the outlet. Increasing the value of χ gives concentration profiles that becomes more and more non-linear indicating a decrease in the nitrate removal efficiency. At high values of χ only the first part of the feed compartment contributes to the nitrate removal.

The overall current efficiency, I_{eff}, gives a measure of the ratio of the current used to remove nitrate. The following definition of I_{eff} is used,

$$I_{eff} = \frac{z_1 F \Delta c_1 h j_0}{\int_0^L (i + \bar{i})\, \mathrm{d}y} \tag{59}$$

where $\Delta c_1 = c_1(\text{Feed}) - c_1(\text{Product})$. In figure 8 the overall current efficiency has been plotted against χ for different Δ-values. The definition of the current efficiency gives very high values of the efficiency at low values of χ where the Donnan dialysis effect removes most of the nitrate without contributing to the current density. This is the reason for the increase in current efficiency as Δ increases for the low χ values. As χ is increased the curves for different Δ-values

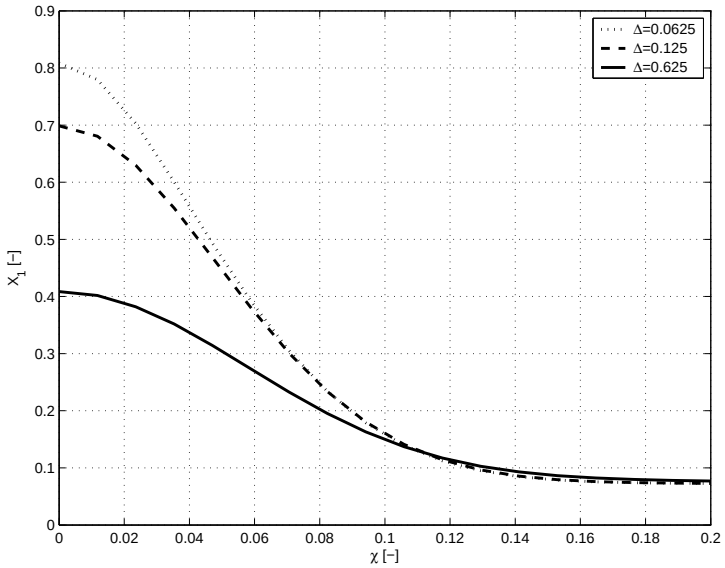

FIGURE 6. The concentration of nitrate at the outlet as a function of χ obtained from simulations of continuous electropermutation. The different curves represent different values of the dimensionless number Δ as indicated in the figure.The value of Z in these simulations was 620.

collapses. This occurs at about the same χ value as the nitrate concentration in the product levels off.

As the value of χ increases the current efficiency decreases. There are several reasons for this decreasing efficiency, the main reason being that the net flux out of the feed compartment decreases as the nitrate concentration decreases.

Also, when studying the nitrate concentration as a function of streamwise position in figure 7, it was found that the nitrate removal efficiency decreases with streamwise position. This can also be shown by plotting the local current efficiency as a function of streamwise position as in figure 9. The local current efficiency is defined by,

$$I_{eff}(y) = \frac{z_1 F[c_1(y-\Delta y) - c_1(y+\Delta y)]hj_0}{[i(y)+\bar{i}(y)]\Delta y}. \tag{60}$$

4.2. *Effect of Z*

The dimensionless numbers Z, defined in equation 50 represents the ratio between the intrinsic concentration of the fixed ion-exchange groups in the textile and the intrinsic concentration of nitrate in the feed. This is an important

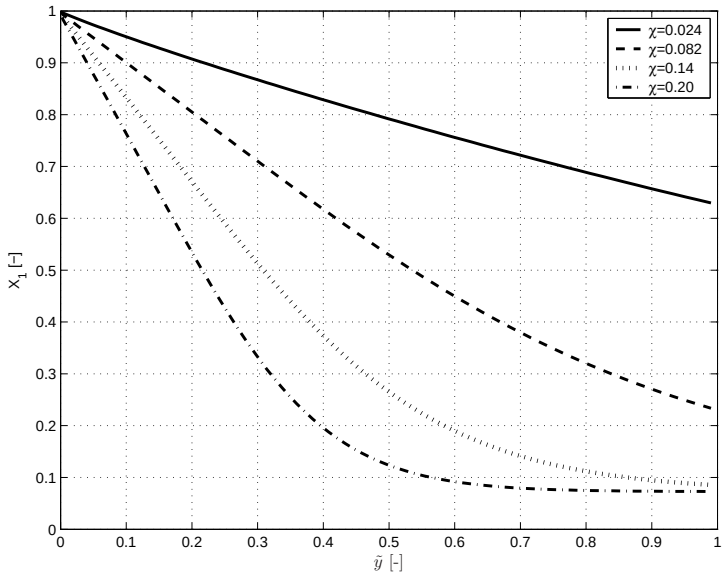

FIGURE 7. The nitrate concentration, in the liquid phase, averaged over the gap between the membranes is plotted as a function of streamwise coordinate for different values of χ. Z=620 and $\Delta = 0.125$.

design parameter when developing a suitable material to be used in an ion-exchange assisted electro-membrane process. It includes the intrinsic volumetric capacity of the ion-exchanger. Increasing the value of Z leads to a higher contribution from the textile-phase to the separation process.

In figure 10 the concentration of nitrate in the product is plotted as a function of χ for different values of Z. The values of ϵ and Δ were held constant in these simulations. This would be the same as using different textiles with the same porosity but with different ion-exchange capacity. It is found that the amount of nitrate removed by Donnan dialysis at $\chi = 0$ increases slowly with Z. This indicates that the mass transfer to the membrane surface in the textile-phase increases with increasing Z. The mass transfer to the membrane surface represents only a small fraction of the resistance for the Donnan dialysis and hence the rather small difference as Z increases.

The importance of the ion-exchange capacity of the textile phase is illustrated when the electric field is applied. As can be seen the nitrate concentration in the product drops dramatically with increasing χ for the simulations with high Z values. When treating a solution containing 100 ppm nitrate, a Z value of 620 represents a textile with a ion-exchange capacity of 1 meq/g, a density of 150 kg/m^3 and a volume fraction of fibers of 0.15. This is close to the characteristics of the anion-exchange textiles developed by with in the Iontex project. The same textile with a capacity of 2.4 meq/g would give a Z value

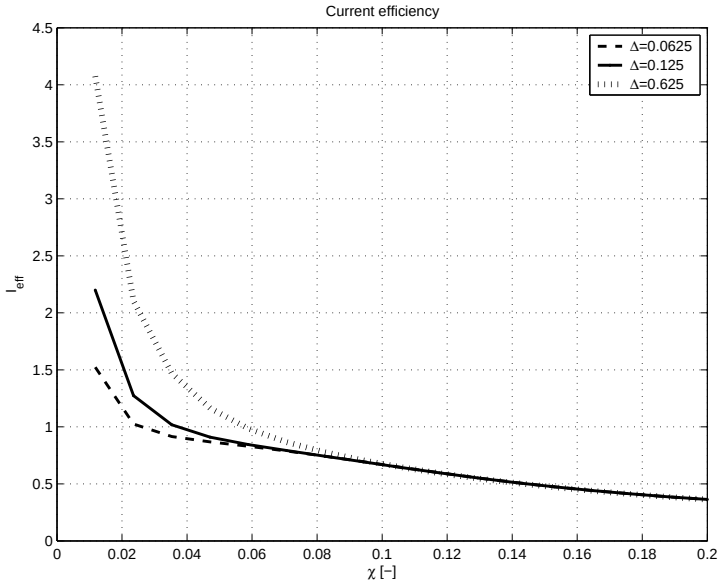

FIGURE 8. The overall current efficiency as a function of χ. The different curves represent simulations with different values of Δ. Z = 620.

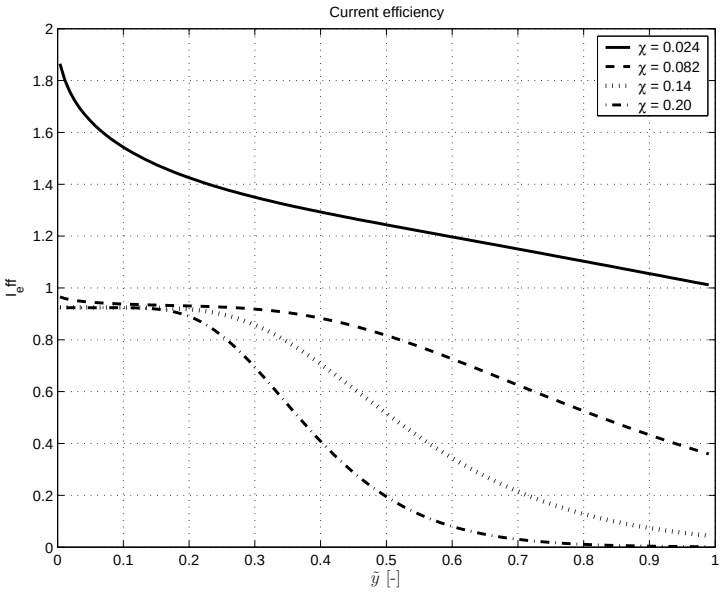

FIGURE 9. The local current efficiency as a function of streamwise position, $\tilde{y}$.

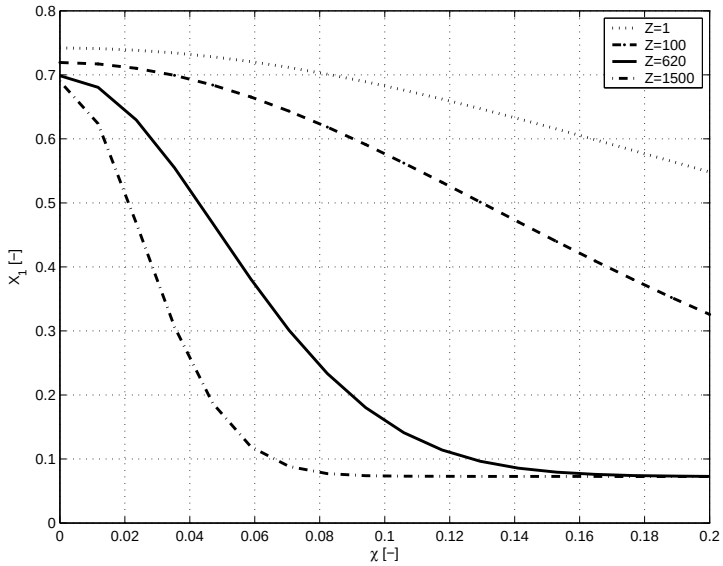

FIGURE 10. The concentration of nitrate in the product as a function of the dimensionless parameter χ, plotted for different values of the dimensionless parameter Z as indicated in the figure. The value of Δ in these simulations was 0.125.

of 1500 which is also represented in figure 10. It is clear that the higher the value of Z the easier it is to remove the nitrate. The nitrate concentration in the product is plotted against the dimensionless power consumption, required to drive the current through the feed compartment, for different values of Z in figure 11. Here the advantage of a high capacity of the β-phase is made clear. A high capacity leads to a lower power consumption for driving an electrical current through the feed compartment. If the capacity of the textile is low then a high value of χ is required to remove a sufficient amount of nitrate. Increasing χ can be done by increasing the potential difference which leads to an increased current density. If then the limiting current density is reached in the liquid phase; water splitting starts to take place and the current efficiency decreases due to the transfer of OH^- over the membrane. This sets a limit to the nitrate removal possible to achieve. Other options to reach high values of χ is to change the dimensions of the feed compartment, or lowering the flow rate. The effect of water splitting is not included in the present model.

5. Conclusions

A macro-homogeneous steady state model for nitrate removal by continuous electropermutation using an ion-exchange textile as conducting spacer has been presented. The macro scale equations are obtained by taking the volume averages of the governing equations at the microscopic scale. To obtain expressions

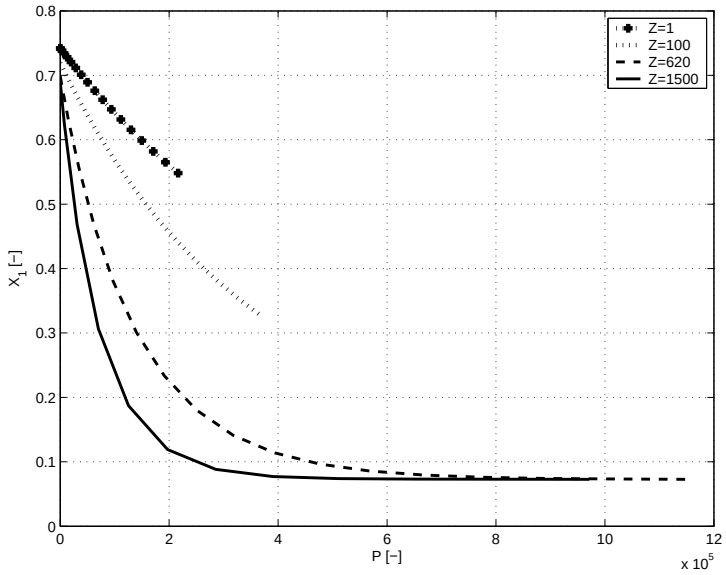

FIGURE 11. The concentration of nitrate in the product as a function of the dimensionless power consumption, plotted for different values of the dimensionless parameter Z as indicated in the figure. The value of Δ in these simulations was 0.125.

for the macro-homogeneous fluxes it was assumed that the two phases that contribute to the mass transfer are in a parallel arrangement. This assumption is a rather hard restriction for the validity of the model. Never the less the model captures the main characteristics of the continuous electropermutation process. The model equations and boundary conditions were made dimensionless and the dimensionless numbers characterising the process were identified. The slender geometry of the modeled domain was used to simplify the equations in the limit when the slenderness ratio $\sigma \to 0$ at the same time as $\vartheta \to 0$ and Pe $\to \infty$. Thus the simplified equations are valid for textiles with small fiber diameters and at flow rates which are not to small. The simplified equations are parabolic rather than elliptic as the complete model equations. The relatively small diameters, order of 10 μm, of the fibers in a typical ion-exchange textile makes it possible to assume ion-exchange equilibrium between the phases. This reduces the number of unknowns in the model from seven to four.

The influence of the most important dimensionless numbers was investigated by solving the model equations numerically. The relative importance of the removal due to the Donnan dialysis effect was found to be described by the dimensionless number Δ defined in equation 42. This was also confirmed by the numerical simulations. The dimensionless number, χ defined in equation 55, is the key number to study when the process parameters are to be optimised. The optimal relation between the applied potential and the flow rate through

the feed compartment can be found by studying, χ and its influence on the process. The third dimensionless number Z which represents the ratio between the intrinsic concentrations in the ion-exchanger and in the solution. Simulations gave that an increased Z value gave a decreased power consumption for driving the current density through the feed compartment.

It has been shown that simulations based on the developed model could give information that would be useful when optimising the process parameters as well as in the stage of designing the equipment. The results from simulations should be compared to experimental results in order to validate the model. A further improvement of the model would be to include the effect of selectivity of the membranes and ion-exchange textile. Furthermore, the effects of the connectivity of the textile material could be included. Including this effect would be useful as to compare different types of spacer material within the model. A rather straight forward improvement of the model would be to make it transient. This would be useful when investigating the effects of disturbances such as e.g. power loss, changes in flow rates etc. on the process.

Acknowledgement

The work was financed by the VINNOVA competence center, FaxénLaboratoriet, with the main industrial partner in this project being Vattenfall AB.

Nomenclature

	Description
Roman letters	
c	concentration [mol/m^3]
d_f	Fibre diameter [m]
D	Diffusion coefficient [m^2/s]
$\mathcal{D}$	Mechanical dispersion tensor [m^2/s]
$\mathcal{D}_\mathcal{L}$	Coefficient of transversal dispersion [m^2/s]
$\mathcal{D}_\mathcal{T}$	dispersion tensor [m^2/s]
F	Faraday's constant F = 96485 [C/mol]
h	Thickness of feed compartment [m]
$\mathbf{i}$	Current density [A/m^2]
$\mathbf{j}$	Superficial velocity [m/s]
L	Length of feed compartment [m]
$\mathbf{n}_{\alpha,\gamma}$	Unit normal vector pointing out of α-phase and into γ-phase [mol/(m^{2}s)]
$\mathbf{N}$	Ionic flux [mol/(m^{2}s)]
R	Gas constant R=8.3145 [J/(mol K)]
S	Sink/source term from ion-exchange rate [mol/(m^{3}s)]
$\mathfrak{S}$	Specific surface area of textile [m^{-1}]
Sc	Schmidts number $\frac{nu}{D}$ [-]
Sh	Sherwoods number $\frac{d}{\delta}$ [-]
T	Temperature [K]
$\mathbf{u}$	Velocity vector [m/s]
u	Ionic mobility [m^{2}mol/(Js)
w	Capacity of the ion-exchange textile [eq/kg]
$\mathcal{V}$	Non dimensional potential scale $\frac{F\phi_0}{RT}$[-]
X	Non dimensional concentration in liquid-phase [-]
Y	Non dimensional concentration in textile-phase [-]
z	Valence of ion [-]
Z	Ratio between the intrinsic concentration scales in both phases $\frac{w\rho_\beta}{\epsilon c_0}$ [-]
κ	Permeability [m^2]
Greek letters	
α	Separation factor [-]
χ	Non dimensional number defined as $\frac{\mathcal{V}}{\sigma^2 Pe}$ [-]
Δ	Non dimensional number $\frac{2D^m c_0^m}{\mu\sigma j_0 c_0}$ [-]
δ	Thickness of diffusion layer around each fiber [m]
δ_c	Thickness of diffusion layer at membrane [m]
ϵ	Volume fraction [-]
κ	Permeability [m^2]
μ	Thickness of membrane [m]

ν	Kinematic viscosity [m^2/s]
ω	concentration of fixed charges in the solid phase [mol/m^3]
Φ	Non dimensional potential [-]
ϕ	potential [V]
ρ	Density [kg/m^3]
σ	Ratio of thickness to length of feed compartment, $\frac{h}{L}$[-]
τ	Tortuosity [-]
θ	Dimensionless number $\frac{\vartheta}{\sigma^2}$ [-]
$\tilde{\delta}$	Dimensionless number $\frac{\delta}{d_f}$ [-]
ϑ	Dimensionless number $\frac{d_f}{L}$ [-]
ξ	Characteristic length of the porous bed [m]
Symbols	
$< .. >$	Superficial volume average
$< .. >_\alpha$	Intrinsic volume average of α-phase.
$< .. >_\beta$	Intrinsic volume average of β-phase.
Subscript	
α	Refers to value in the liquid-phase
β	Refers to value in the textile-phase
γ	Refers to value in the stagnant layer around the fibers
cc	Refers to value in the concentrate compartment
mem	Refers to value in the membranes
i	Specie i
1	NO_3^-
2	Cl^-
3	Na^+
Superscript	
*	Value taken at phase-interface
'	Deviation from volume averaged
-	Refers to value in the textile-phase
$\sim$	Non dimensional variable
m	Refers to value in the membranes

References

Bear, J. 1988 *Dynamics of Fluids in Porous Media*. Dover, iSBN 0-486-65675-6.

Bird, R., Stewart, W. & Lightfoot, E. 2002 *Transport Phenomena*, 2nd edn. Wiley.

Dejean, E. 1997 Electrodesionisation sur textiles echangeurs d'ions. PhD thesis, Universitet Montpellier II.

Dejean, E., Laktionov, E., Sandeaux, J., Sandeaux, R., Pourcelly, G. & Gavach, C. 1997 Electrodeionization with ion-exchange textile for the production pf high resistivity water: Influence of the nature of the textile. *Desalination* **114**, 165–173.

Dejean, E., Sandeaux, J., Sandeaux, R. & Gavach, C. 1998 Water demineralization by electrodeionization with ion-exchange textiles. comparison with conventional electrodialysis. *Separation Science and Technology* **33** (6), 801–818.

Dullien, F. 1992 *Porous Media, Fluid Transport and Pore Structure*, 2nd edn. Academic Press.

Elattar, A., Elmidaoui, A., Pismenskaia, N., Gavach, C. & Pourcelly, G. 1998 Comparison of transport properties of monovalent anions through anion-exchange membranes. *Journal of Membrane Science* **143**, 249–261.

Ezzahar, S., Cherif, A., Sandeaux, J., Sandeaux, R. & Gavach, C. 1996 Continuous electropermutation with ion-exchange textiles. *Desalination* **104**, 227–233.

Glueckauf, E. 1959 Electro-deionisation through a packed bed. *British Chemical Engineering* pp. 646–651.

Greenkorn, R. 1983 *Flow Phenomena in Porous Media*. Dekker.

Helfferich, F. 1995 *Ion Exchange*. Dover, iSBN 0-486-68784-8.

Johann, J. & Eigenberger, G. 1993 Elektrodialytische regenerierung von ionenaustauscher-harzen. *Cem.-Ing.-Tech.* **1**, s.75–78.

Koch, D. 1996 Hydrodynamic diffusion near soid boundaries with applications to heat and mass transport into sheard suspensions and fixed-fibre beds. *J. Fluid Mech.* **318**, 31–47.

Kourda, N. 2000 Électropermutation sur textiles Échangeurs de cations. PhD thesis, Universitet Montpellier II.

Laktionov, E., Dejean, E., Sandeaux, J., Gavach, C. & Pourcelly, G. 1999 Production of high resistivity water by electrodialysis. influence of ion-exchange textiles as conducting spacers. *Separation Science and Technology* **34**, 69–84.

Mulder, M. 1996 *Basic Principles of Membrane Technology*. Kluwer Academic Publishers.

Newman, J. S. 1991 *Electrochemical Systems*, 2nd edn. Prentice Hall, iSBN: 0-13-248758-6.

Petruzzelli, D., Kalinitchev, A., Soldatov, V. S. & Trivavanti, G. 1995 Chloride/sulfate ion exchange kinetics on fibrous resins. two independent models for film diffusion control. *Ind. Eng. Chem. Res.* **34**, 2618–2624.

Rubinstein, I. 1977 Electrodialysis in a dispersed system. *J.Chem.Soc.,Faradays Trans.* **73** (2), 528–544.

Salem, K., Sandeaux, J., Molénat, J., Sandeaux, R. & Gavach, C. 1995 Elimination of nitrate from drinking water by electrochemical membrane processes. *Desalination* **101**, 123–131.

Schlöel, R. & Schöedel, U. 1955 Über das verhalten geladener porenmembranen bei stromdurchgang. *Z.phys.Chemie* p. S.372.

Thate, S. 1998 *Continuous ElectroDeIonization(CEDI)- A combination of electrodialysis and ion-exchange.*. Part of Advanced Course on Membrane Technology-Electro-membrane Processes, CIVT, Stuttgart.

Verbeek, H., Fürst, L. & Neumeister, H. 1998 Digital simulation of an electrodeionization process. *Computers chem. Eng.* **22**, 913–916.

Walters, W., Weiser, D. & Marek, L. 1955 Concentration of radioactive aqueous waste, electromigration through ion-exchange membranes. *Industrial and Engineering Chemistry* **47** (1), 61–67.

Whitaker, S. 1999 *The Method of Volume Averaging*. Kluwer Academic Publisher, iSBN 0-7923-5486-9.

WHO 2004 Guidlines for drinking water quality; recomendations i, geneva. 3rd Edition.

Wilson, E. & Geankoplis, C. 1966 Liquid mass transfer at very low reynolds numbers in packed beds. *Ind.Eng.Chem.Fund.* **5** (9).

Paper 3

3

Nitrate Removal by Continuous Electropermutation using Ion-Exchange Textile Part II: Experimental Investigation

By Carl-Ola Danielsson[1], Anna Velin[2], Mårten Behm[3] & Anders Dahlkild[1]

Water with nitrate concentrations above 100 ppm is treated with continuous electropermutation. The feed compartment of the electropermutation cell is filled with an anion-exchange textile. Experiments with and without textile are compared and the influence of the textile is discussed. The influence of pressure differences over the membranes is investigated and the importance of establishing a good contact between the membranes and the textile spacer is pointed out. The experimental results are compared to model predictions as to validate the model.

1. Introduction

Increased levels of nitrate in the groundwater has made many wells unsuitable as drinking water sources. There are a number of available techniques for removal of nitrate for production of drinking water (Kapoor & Viraraghavan 1997), such as biological methods, ion-exchange and electrodialysis. In this paper a electromembrane technique called electroextraction or continuous electropermutation (CEP) (Ezzahar *et al.* 1996; Basta *et al.* 1998; Kourda 2000), using anion-exchange textile as conducting spacer, will be investigated experimentally.

The principles of continuous electropermutation are illustrated in figure 1. The water to be treated is passed through the feed compartment of an electromembrane cell. The feed compartment is separated from the concentrate compartments by anion permeable membranes. Under the influence of an applied electric field the anions in the feed water are replaced by anions present in the concentrate compartment. A product with low nitrate content as well as a more concentrated nitrate effluent suitable for e.g. electro-reduction (Paidar *et al.* 1999) can be obtained with a suitable composition of the concentrate solution. As long as the relative nitrate concentration in the concentrate solution

[1]Department of Mechanics, KTH, SE-100 44 Stockholm, Sweden.
[2]Vattenfall Utveckling AB, SE-100 00 Stockholm, Sweden.
[3]Department of Chemical Engineering and Technology, KTH, SE-100 44 Stockholm, Sweden.

is kept low it is possible to build electropermutation stack with a repeating unit of two compartments.

The low conductivity of the feed solution leads to a high power consumption as well as limiting the current density that can be used. In the present study a new non-woven textile with strong anion exchange properties was used as conducting spacer in the feed compartment. The ion-exchange textile used was developed within the EU-funded research project Iontex (Schoebesberger *et al.* 2004). The fibers in the textile were provided by Lenzing, Austria and the needle punched non-woven textile was produced by Orsa, Italy. IFTH, France, introduced the functional groups, providing the ion-exchange capacity, by electron beam grafting.

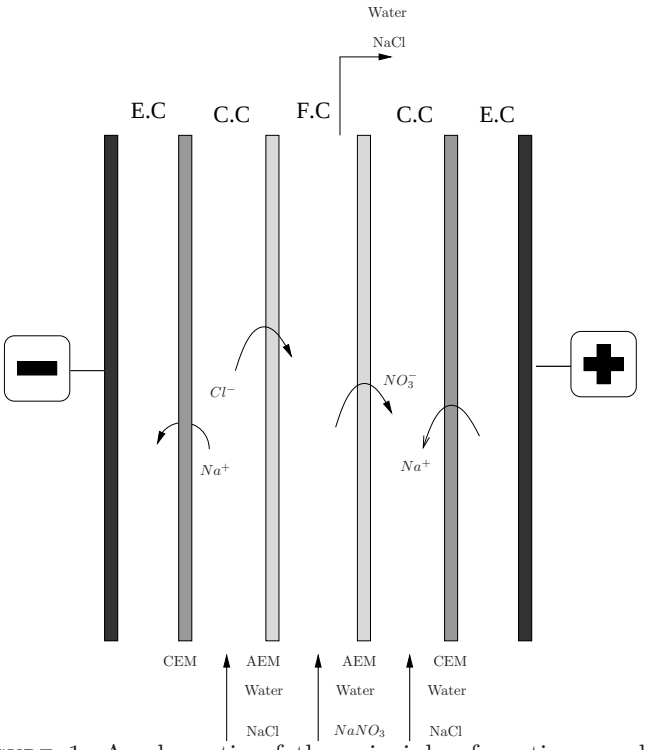

FIGURE 1. A schematic of the principle of continuous electropermutation used for nitrate removal. The nitrate in the feed water is replaced by another anion, in this case chloride, under the influence of an applied electric field.

The purpose of the work presented in this paper is to investigate the performance of the new anion-exchange textile as a conducting spacer. Experiments on synthetic nitrate solutions have been conducted with and without

textile incorporated in order to study the influence of the textile. Furthermore, the performed experiments aimed to validate a mathematical model developed within the Iontex project. The steady state model is described in a previous paper (Danielsson *et al.* 2004*b*).

2. Experimental

The Neosepta standard grade membranes AMX and CMX from Tokuyama Soda was used to separate the compartments. The characteristics of the textile and membranes used are given in table 1.

	Textile	AMX	CMX
Type	Anion exchange Textile	Anion permeable membrane	Cation permeable membrane
Thickness [mm]	3.0-3.3	0.16-0.18	0.17-0.19
Capacity [meq/g]	0.5-0.7	1.4-1.7	1.5-1.8

TABLE 1. Properties of ion-exchange textile and membrane used.

The ion-exchange textile used is not designed to be selective for nitrate. The selectivity of a similar textile grafted by IFTH was investigate by Passounaud *et al.* (2000). They found that the selectivity coefficient between nitrate and chloride, $K(NO_3^-/Cl^-)$, was about 2. The selectivity coefficient is defined as,

$$K(NO_3^-/Cl^-) = \frac{[\overline{NO_3^-}][Cl^-]}{[NO_3^-][\overline{Cl^-}]} \tag{1}$$

where the overbars indicates concentrations of ions bound to the textile at equilibrium.

2.1. *Equipment*

A photo of the experimental setup is presented in figure 2. The cell used in this study was composed of five compartments separated by ion-exchange membranes, a schematic is presented in figure 1. The electrode compartments were taken from an ElectroSynCell (Carlsson *et al.* 1983). The concentrate and feed compartments were built up by inhouse developed frames (Danielsson *et al.* 2004*a*) with a thickness of 2 mm each. Together with 0.5 mm flat gaskets, made from EPDM, on each side the compartments were 3 mm thick. Net-type spacers were used to provide mechanical support to the membranes. For the cases when the textile was incorporated in the feed compartment the net-type spacer was replace by the textile. The active membrane area of the cell was 0.04 m^2. The cell used in the present study was a full scale cell. Stacks of cells in series can be constructed as to obtain a desired production capacity.

A DSA electrode, titanium coated with iridium, was used as anode and a nickel electrode as cathode.

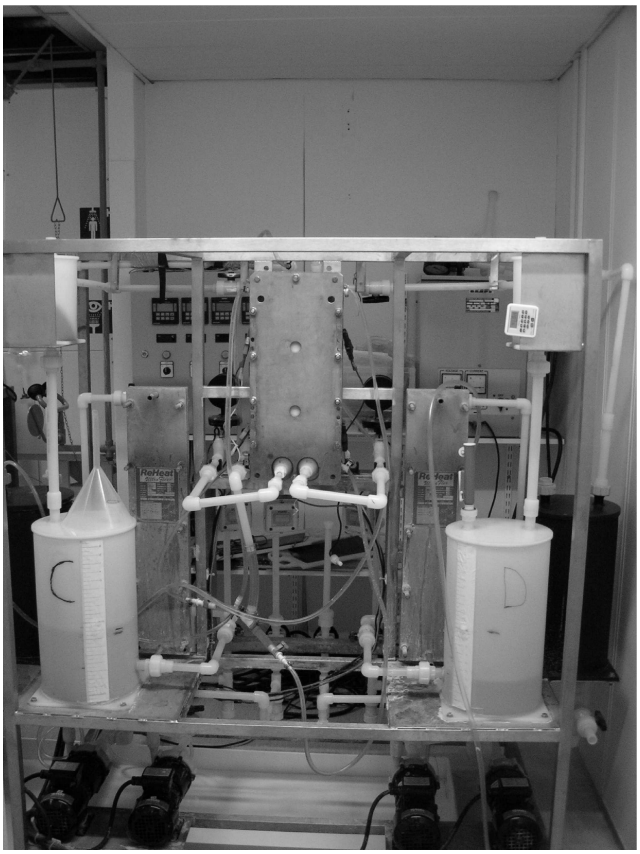

FIGURE 2. A photo of the experimental setup used in the investigation of continuous electropermutation.

The concentrations of nitrate, chloride and sulphate were determined by ion chromatography, using the Dionex Ag17-As17 columns, and pH was measured with a pH-electrode from Radiometer.

2.2. *Operating conditions*

Before the textile was introduced into the cell it was washed carefully with deionised water to remove any excess chemicals remaining from the grafting process, and it was turned into chloride form by treating the textile with a sodium chloride solution.

The operating conditions used are summarised below.

- A synthetic sodium nitrate solution served as feed. The level of nitrate in the feed was 105 ppm which corresponds to 1.7 mM.
- A single pass mode of operation was used for the feed.

- The solution in the concentrate compartments (C.C) was 20 liters of 0.2 M sodium chloride which was recirculated.
- The solution in the electrode compartments (E.C) was 10 liters of 0.3 M sodium sulphate which was recirculated.
- The current was varied between 0 and 1 A corresponding to a average current density of 0 up to 25 A/m^2.
- The pressure drop over the different compartments were adjusted according to the different experimental cases presented in table 2.

From preliminary experiments it was found that at least 30 min of operation was needed to reach steady state. Samples were taken from the outlet of the feed compartment after 45 and 60 min, in connection to this the flow rate through the feed compartment was measured.

Cases	A	B	C	D	E
Spacer	Textile	Net-type	Textile	Textile	Net-type
ΔP F.C [bar]	0.17	0.13	0.15	0.30	0.10
ΔP E.C & C.C [bar]	0.17	0.15	0.25	0.40	0.20
Flow rate [m/s]	0.18	0.18	0.04	0.12	0.12

TABLE 2. The different test cases. F.C refers to feed compartment. E.C and C.C refers to electrode compartments and concentrate compartments respectively.

3. Results and Discussion

In the first series of experiments the same pressure drop were used over all compartments. The pressure drop was adjusted so that the same flow rate was obtained both with and without the textile. With the textile the pressure drop applied was 0.17 bar, case A, and without the textile it was 0.13 bar, case B. This gave a superficial flow velocity of 0.017 m/s through the feed compartment.

In figure 3 the concentrations of nitrate and chloride in the product are plotted as a function of the average current density for cases A and B. The initial concentration of nitrate in the feed was 1.7 mM.

Already at zero current a significant nitrate removal has been accomplished due to Donnan dialysis. The driving force for Donnan dialysis is the concentration difference of chloride over the membranes. As the current density is increased the nitrate concentration in the product remains almost unchanged. In case A with the textile the concentration decreases to about 1 mM at 25 A/m^2 and in case B it goes down to about 1.2 mM at the same current density. It seem that increasing the current density does not increase the nitrate removal rate. The concentration of chloride in the product, however, increases with the average current density as is seen to the right in figure 3.

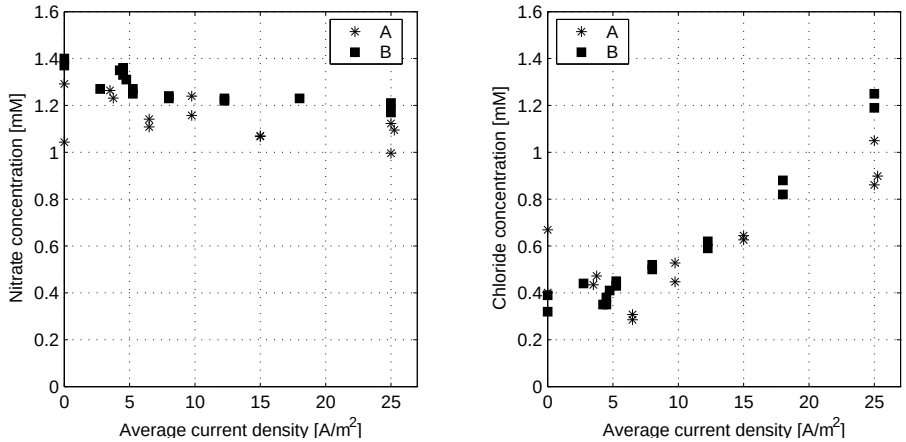

FIGURE 3. Nitrate and chloride concentrations as function of average current density. In case A the ion-exchange textile was incorporated and in case B a PE net-type spacer was used.

The poor improvement of nitrate removal as the current density increases is thought to be explained by water splitting taking place at the membrane interface. This is supported by the change in pH of the product which is plotted in figure 4. The pH of the product drops as the current density is increased. This indicates that water splitting takes place in the feed compartment and the generated hydroxide ions are transported out of the feed compartment instead of nitrate. The pH change seem to be somewhat less for case A in which the textile is used in the feed compartment. The difference between cases A and B is however not significant. This would indicate that the ion-exchange textile behaves rather poorly. One possible explanation for the poor performance of

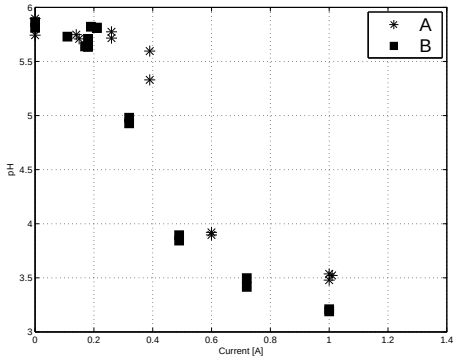

FIGURE 4. pH in product as a function of average current density. Cases A is with ion-exchange textile incorporated and case B is without textile.

the textile is the creation of preferential flow paths between the membrane and the ion-exchange textile. This problem was described in the thesis of Dejean (1997), and would lead to insufficient contact between the membrane and the textile.

In the experimental setup used there was no way to determine the pressure difference over the membranes, only the pressure drop over each compartment could be determined. In order to study the importance of the pressure drops over the different compartments; the pressure drop over the concentrate and electrode compartments was increased in case C. The idea was to ensure that a good contact was established between the membranes and the textile by increasing the pressure outside of the feed compartment. The flow velocity through the feed compartment obtained in case C decreased to 4 mm/s. This indicates that resistance for the flow in the feed compartment increased as consequence of the increased pressure outside of the feed compartment. As can be seen in figure 5 about 90% of the nitrate was removed by Donnan dialysis due to the low flowrate. Applying the electric field seem unnecessary.

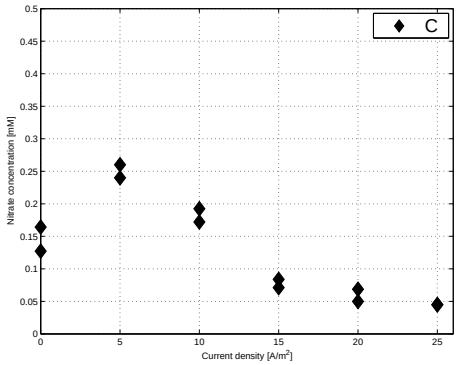

FIGURE 5. Nitrate concentration in product as function of current density for case C. Ion-exchange textile is incorporated in the feed compartment and the linear velocity of the water through the cell is 4 mm/s.

The pressure drop over the feed compartment was increased as to obtain a higher flow rate. In case D, with textile incorporated, and E, without textile, the linear flow velocity was 1.2 cm/s. In both case D and E the pressure drop over the feed compartment was 0.1 bar lower than over the other two compartments to provide good contact between the textile and the membrane in case D. The concentrations of nitrate and chloride in the product for these cases are plotted against the average current density in figure 6.

The nitrate removal by Donnan dialysis is much higher with textile incorporated compared to without textile. This suggests that the textile improves the mass transfer to the membrane surface. Results obtained from simulations

showed that the capacity of the ion-exchange textile only had a very weak influence on the nitrate removal by Donnan dialysis. However, the introduction of the textile material makes the diffusion layer in the liquid much thinner which will contribute to an increased mass transfer to the membrane surface. In a paper by Berdous & Akretche (2002) it is claimed that the efficiency of Donnan dialysis is improved with ion-exchange textile incorporated as a result of a reduced osmotic pressure difference over the membrane. This could not be by the model since the convective transport through the membrane was neglected in the model.

The nitrate removal increased with the current density in case D, as can be seen in figure 6 and at 25 A/m^2 the nitrate concentration is as low as 0.25 mM (15 ppm), which is well below the limiting values allowed for drinking water purposes (European Community 1998; WHO 2004). It is expected that the pH change should be less in case D compared with case A, in which the textile was also incorporated, since nitrate is removed instead of hydroxide. That this is the case is seen in figure 7 where the pH for case D and E are plotted as a function of the average current density. The results for case E are almost

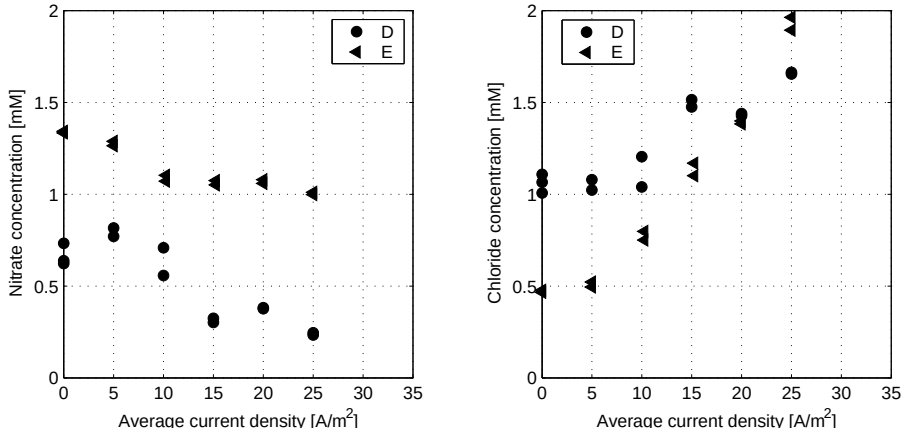

FIGURE 6. The concentration of nitrate and chloride in the product as a function of average current density for cases D and E

identical with those of case B. Thus the differences between cases A and D can not be explained by any transport related to the pressure difference over the membranes.

It seems that it is important to establish good contact between the conducting spacer and the membranes. Increasing the pressure in the concentrate and electrolyte compartments is not the ideal way to ensure contact between membrane and textile. A pressure difference over the membrane can lead to a convective flow into the feed compartment which would make nitrate removal

more difficult. In electrodeionisation one usually fills both the concentrate and dilute compartments with conducting spacers, this provides the same hydrodynamic conditions on both sides of the membrane and makes it more convenient to control the pressure difference over the membranes. In the electropermutation process the conductivity of the solution in the concentrate compartment is high. Introduction of a conducting spacer such as the ion-exchange textile into the concentrate compartment leads to a increased power consumption. A better way to minimise the risk for the creation of preferential flow paths between the membrane and the textile would be to provide a better mechanical support to the membranes.

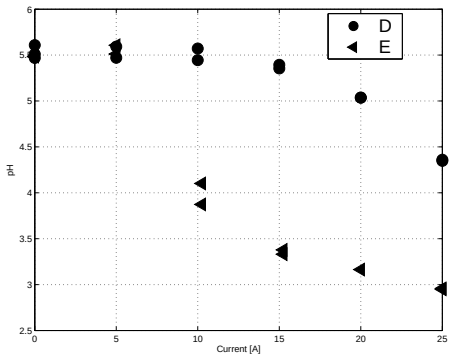

FIGURE 7. The pH of the product as a function of average current density for cases D and E

In figure 8 the removed nitrate, introduced chloride and removed hydroxide are plotted against the current density for cases D and E. The removed hydroxide is calculated from the change in pH over the feed compartment. The amount of hydroxide transferred away from the feed compartment in case E is significantly higher than in case D. This is also reflected in the net introduction of chloride which is higher in case E. In case D a higher degree of the current is carried by chloride ions, that are transferred through the feed compartment without leading to a net increase of the chloride concentration. The total ionic strength of the product is higher for case E due to the water splitting taking place, giving a production of ions in the feed compartment.

Increasing the current density above 10 A/m^2 in case E does not result in an increased nitrate removal. Instead water splitting takes place and hydroxide ions are removed from the feed compartment. Introducing the ion-exchange textile however makes it possible to increase the current density to 25 A/m^2 before water splitting starts to become important.

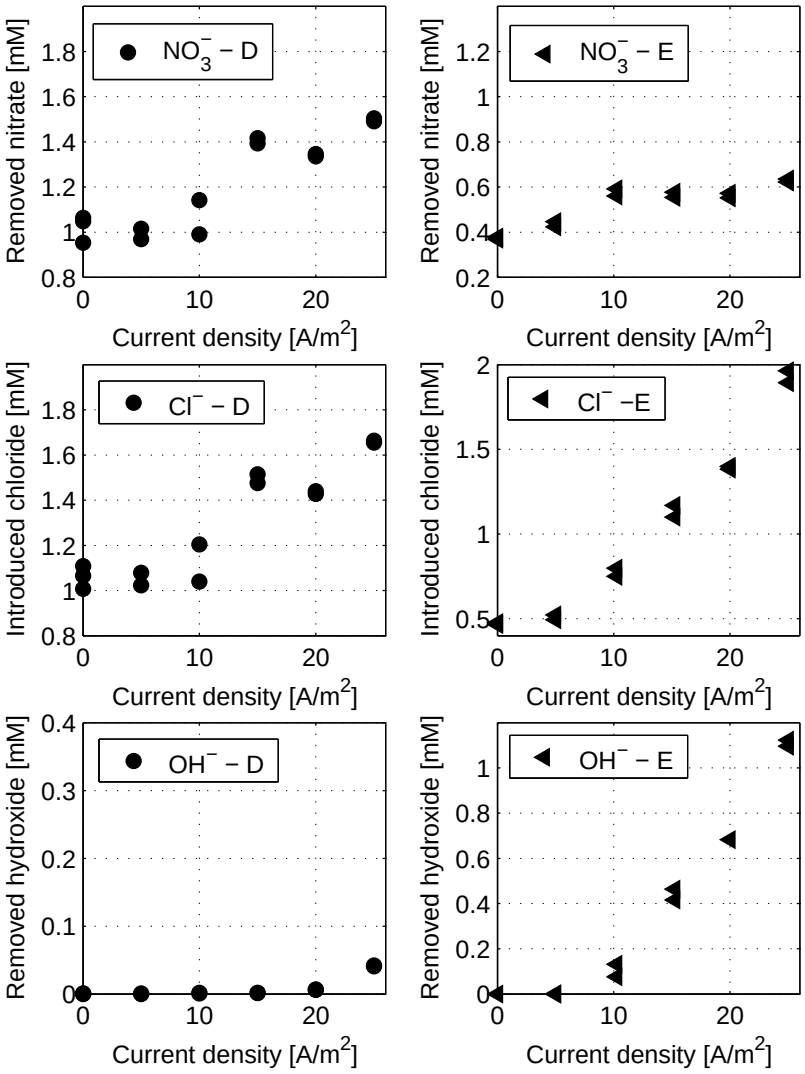

FIGURE 8. Changes in concentration over the feed compartment for case D with textile incorporated to the left. Case E without textile to the right. The amount of nitrate removed is plotted at the top. In the center the increase in chloride concentration is plotted and at the bottom the decrease in hydroxide concentration is plotted against the average current density. The average velocity of the water in both case D and E was 1.2 cm/s

The power consumption, required to drive the electrical current through the whole experimental setup, for cases D and E are plotted in figure 9 as a function of the average current density. It is clear that the incorporation of the textile as conducting spacer reduces the power consumption for driving the current. The power consumption plotted in figure 9 includes the losses at the electrodes which might be neglected in a large stack with up to 50 elementary electropermutation cells in between each pair of electrodes. The

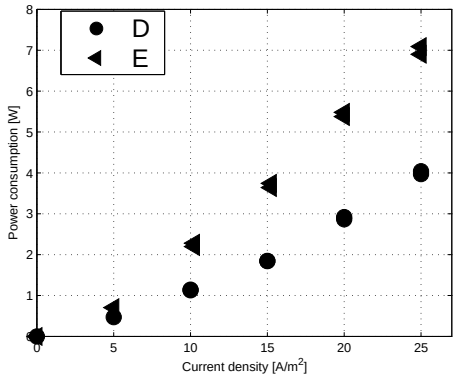

FIGURE 9. Power consumption of the electropermutation process

total power consumption includes the contribution from the pumps forcing the flow through the different compartments. The increase in resistance with the textile incorporated leads to a higher power consumption for pumping and whether the total power consumption is reduced or not needs to be evaluated.

The experiments in case D seem to best represent the assumptions of the model presented a previous paper (Danielsson *et al.* 2004*b*). The model predictions are plotted together with the experimental results in figure 10. The model parameters used to obtain the results in figure 10 are given in appendix A. There are a number of parameters in the model that are unknown but physically reasonable values have been assumed. The model predictions agree well with the experimental results. Water splitting is not included in the present model. It is therefore expected that the nitrate concentration should be somewhat lower in the model predictions at the current densities above the water splitting.

4. Conclusions

Experiments were conducted with a continuous electropermutation system with a new anion-exchange textile incorporated as conducting spacer to remove nitrate. The influence of using the ion-exchange textile as conducting spacer was investigated by conducting experiments with and without ion-exchange textile in the feed compartment. It was shown that an significant increase in the nitrate removal as well as an decrease in power consumption was obtained by

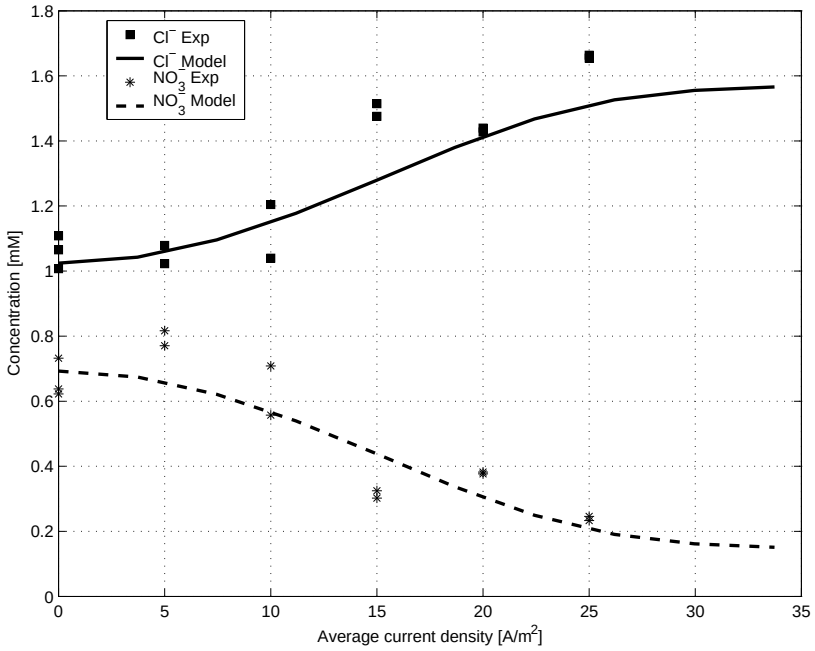

FIGURE 10. The model predictions for the outlet concentrations of chloride and nitrate plotted against the average current density together with the experimental results.

using the ion-exchange textile, developed in the Iontex project, as a conducting spacer. From an initial nitrate concentration of 1.7 mM in the feed water a product stream with 20 mM of nitrate could be obtained in a single pass mode of operation with an applied current density of 25 A/m^2. The nitrate level in the product stream was well below the limiting value for drinking water. The flow rate used corresponded to a production capacity of 20 l/h/unit cell. A stack with 50 elementary cell would be able to treat 1 m^3 of water per hour.

The importance of a satisfactory contact between the membrane and the ion-exchange textile was pointed out. If the pressure in the feed compartment is too high compared to the adjacent concentrate compartments, preferential flow paths can be created between the membranes and the textile. The advantage of using the ion-exchange textile is then reduced and the process behaves very similar to the case with no textile incorporated. When the pressure drop over the concentrate and electrolyte compartments were increased as to ensure contact between membrane and textile a dramatically improved nitrate removal was obtained.

Incorporation of the ion-exchange textile improved the nitrate removal by Donnan dialysis. Nitrate removal by Donnan dialysis is however rather slow compared to continuous electropermutation.

Comparisons between predictions of a previously presented mathematical model and the experimental data were made as to validate the model and the assumptions made. A good agreement between the experimental results and the model predictions was obtained. This comparison was made as to validate the model.

Nitrate removal for drinking water production, with continuous electropermutation using ion-exchange textile shows a great potential. A continued development of the ion-exchange textiles will hopefully provide textiles with higher capacity and thus better conductivity, which will further reduce the power consumption.

Acknowledgement

The work was financed by the VINNOVA competence center, FaxénLaboratoriet, with the main industrial partner in this project being Vattenfall AB.

Nomenclature

	Description
Roman letters	
c	concentration [mol/m^3]
d_f	Fibre diameter [m]
D	Diffusion coefficient [m^2/s]
F	Faraday's constant F = 96485 [C/mol]
h	Thickness of feed compartment [m]
i	Current density [A/m^2]
j	Superficial velocity [m/s]
L	Length of feed compartment [m]
R	Gas constant R=8.3145 [J/(mol K)]
S	Sink/source term from ion-exchange rate [mol/(m^{3}s)]
T	Temperature [K]
u	Velocity vector [m/s]
w	Capacity of the ion-exchange textile [eq/kg]
z	Valence of ion [-]
Z	Ratio between the intrinsic concentration scales in both phases $\frac{w\rho_\beta}{\epsilon c_0}$ [-]
Greek letters	
α	Separation factor [-]
χ	Non dimensional number defined as $\frac{\mathcal{V}}{\sigma^2 Pe}$ [-]
Δ	Non dimensional number $\frac{2D^m c_0^m}{\mu\sigma j_0 c_0}$ [-]
δ	Thickness of diffusion layer around each fiber [m]
δ_c	Thickness of diffusion layer at membrane [m]
ϵ	Volume fraction [-]
κ	Permeability [m^2]

μ	Thickness of membrane [m]
ν	Kinematic viscosity [m^2/s]
ω	concentration of fixed charges in the solid phase [mol/m^3]
ϕ	potential [V]
ρ	Density [kg/m^3]
σ	Ratio of thickness to length of feed compartment, $\frac{h}{L}$[-]
τ	Tortuosity [-]
ξ	Characteristic length of the porous bed [m]
Subscript	
α	Refers to value in the liquid-phase
β	Refers to value in the textile-phase
cc	Refers to value in the concentrate compartment
mem	Refers to value in the membranes
i	Specie i
1	NO_3^-
2	Cl^-
3	Na^+
Superscript	
*	Value taken at phase-interface
-	Refers to textile-phase
m	Refers to value in the membranes

Appendix A

Geometry and Operation Conditions	
h	3 [mm]
L	0.3 [m]
σ	10^{-2} [-]
T	298 [K]
j	0.012 [ms^{-1}]
ϕ_0	0-4 [V]
c_{01}	1.7 [mM]
X_{01}	1 [-]
X_{02}	0.1 [-]
X_{03}	1.1 [-]
X_{01}^m	0.1 [mM]
X_{02}^m	0.9 [M]
ϵ_α	0.85 [-]
ϵ_β	0.15 [-]
Textile and membrane parameters	
Z	410 [-]
d_f	18 [μm]
μ	170 [μm]
c_{mem}^m	1 [M]
α_2^1	2 [-]
α_2^{m1}	1.5 [-]
Physical parameters	
D_1	$1.902 \cdot 10^{-9}$ [m^2s^{-1}] Newman (1991)
D_2	$2.032 \cdot 10^{-9}$ [m^2s^{-1}] Newman (1991)
D_3	$1.334 \cdot 10^{-9}$ [m^2s^{-1}] Newman (1991)
D_1^m	$2.8 \cdot 10^{-11}$ [m^2s^{-1}] Elattar *et al.* (1998)
D_2^m	$3.9 \cdot 10^{-11}$ [m^2s^{-1}] Elattar *et al.* (1998)
z_1	-1 [-]
z_2	-1 [-]
z_3	1 [-]

TABLE 3. Parameter values used in the simulations.

References

BASTA, K., ALIANE, A., LOUNIS, A., SANDEAUX, R., SANDEAUX, J. & GAVACH, C. 1998 Electroextraction of Pb^2+ ions from diluted solutions by a process combining ion-exchange textiles and membranes. *Desalination* **120**, 175–184.

Berdous, D. & Akretche, D. 2002 Recovery of metals by donnan dialysis with ion-exchange textiles. *Desalination* **144**, 213–218.

Carlsson, L., Sandegren, B., Simonsson, D. & Rihovsky, M. 1983 Design and performance of a modular, mulit-purpose electrochemical reactor. *J.Electrochem.Soc.* p. 342.

Danielsson, C.-O., Dahlkild, A., Velin, A. & rten Behm, M. 2004*a* Flow distribution study of new electrodialysis module. In *Continuous Electropermutation using Ion-Exchange Textile*. KTH, Mekanik, tRITA-MEK 2004:14.

Danielsson, C.-O., Dahlkild, A., Velin, A. & rten Behm, M. 2004*b* Nitrate removal by continuous electropermutation using ion-exchange textile part i: Modeling. In *Continuous Electropermutation using Ion-Exchange Textile*. KTH, Mekanik, tRITA-MEK 2004:14.

Dejean, E. 1997 Electrodesionisation sur textiles echangeurs d'ions. PhD thesis, Universitet Montpellier II.

Elattar, A., Elmidaoui, A., Pismenskaia, N., Gavach, C. & Pourcelly, G. 1998 Comparison of transport properties of monovalent anions through anion-exchange membranes. *Journal of Membrane Science* **143**, 249–261.

European Community 1998 Council directive of 3 november 1998. Official J.Europ.Commun., L330, 05/12/1998 P. 0032 - 0054.

Ezzahar, S., Cherif, A., Sandeaux, J., Sandeaux, R. & Gavach, C. 1996 Continuous electropermutation with ion-exchange textiles. *Desalination* **104**, 227–233.

Kapoor, A. & Viraraghavan, T. 1997 Nitrate removal from drinking water - review. *Journal of Environmental Engineering* pp. 371–380.

Kourda, N. 2000 Électropermutation sur textiles Échangeurs de cations. PhD thesis, Universitet Montpellier II.

Newman, J. S. 1991 *Electrochemical Systems*, 2nd edn. Prentice Hall, iSBN: 0-13-248758-6.

Paidar, M., Rousar, I. & Bouzek, K. 1999 Electrochemical removal of nitrate ions in waste solutions after regeneration of ion exchange columns. *Journal of Applied Electrochemistry* **29**, 611–617.

Passounaud, M., Bollinger, J., Serpaud, B. & Lacour, S. 2000 Water nitrate removal with ion-exchanger grafted textiles. *Environmental Technology* **21**, 745–753.

Schoebesberger, H., Einzmann, M., Schmidtbauer, J., Gayrine, P. & Martinetti, R. 2004 Iontex-viscose fibers with ion exchange properties. *Chemical Fibes International* **54** (2), 101–111.

WHO 2004 Guidlines for drinking water quality; recomendations i, geneva. 3rd Edition.